Development of a wear test for the evaluation of cemented carbides used in rotary drilling applications

Carlos Filipe Afonso Moura

Final Project – Mechanical Engineering Master

September 2008 – February 2009

Fagersta, Sweden – Porto, Portugal

Abstract

The appearance of cemented carbides has revolutionized the rock drilling industry. Nowadays, virtually all the rock drilling bits use cemented carbide inserts. Their advantageous mechanical characteristics enable the possibility of drilling extremely hard grounds at high penetration rates.

Atlas Copco Secoroc AB is the world leader in the production of consumable rock drilling equipment. Given its commitment to continuous research and development, the company is constantly trying to find new ways to improve its products.

Within this ambit, the following project was done.

Its main purpose was the development of a half-field test rig. This rig would be used to simulate the real conditions found in rotary crushing drilling in order evaluate the wear behaviour of different cemented carbide grades.

The dynamics of the rock drilling technique and its influence on wear mechanisms were analyzed. The evaluation of worn drill bits was also done in order to gain understanding about these mechanisms and how to simulate them most effectively.

Consequently, design specifications for the half-field test were settled. With all the different components duly chosen and designed, the project for the complete test rig was done.

Acknowledgements:

In Sweden, I would like to thank

Atlas Copco Secoroc AB for this great opportunity

Lars M. Karlsson for supervising this project, for the constant availability and all the support

Claes Tigerstrand for choosing me for this position

The Materials R&D team for the daily company

The Top-Hammer team for all the patience to answer my infinite questions

The workshop team for borrowing me all the tools I needed

The cemented carbides production team for showing me how things work

The human resources team for providing all the great conditions

In Portugal, I would like to thank

FEUP for the excellence of its education throughout all these years

Antonio Monteiro Batista for all the supervision at the faculty

Paulo Tavares de Castro for supporting this project

And finally the Eramus-Internship program without which this project would not be possible

Contents

1 - Introduction

Ground drilling has been done for over 3000 years. Since the pulley system used in the ancient China [fig1], the drilling technique has been constantly developing. The increasing demands of mining and construction industries have stimulated this development. Nowadays, the state-of-art makes it possible to drill oil wells in the middle of the ocean at high depths, to blast holes in the extremely hard grounds of iron ore mines. Though, most of these capacities would not be possible without the appearance of cemented carbides. These hard materials have made it possible to build tools for drilling in virtually any sort of ground.

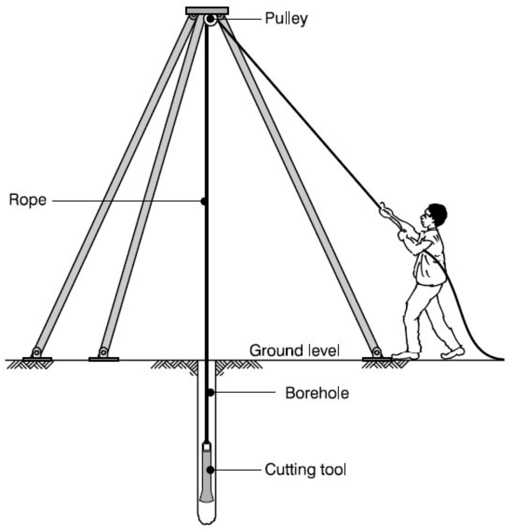

[fig1] – Pulley percussive drilling system used in the ancient China 3000 years ago

Given its importance, these hard-metals have been intensively studied in the last fifty years. Several authors have contributed for this purpose, and extensive information about this subject can be found in the literature. Despite this fact, a lot of work remains to be done in the field of the wear testing. There is no standard wear test to simulate real drilling conditions, thus, most of the companies have to rely on the basic material testing or develop their own testing methods.

2 - Cemented carbides

Cemented carbides (or hardmetals) are composite materials, obtained by powder metallurgy. From a technical point of view, tungsten-carbide (WC) based hardmetals are by far the most important group [3]. One of the most common associations is the WC-cobalt cemented carbide. It is a metal matrix composite where tungsten carbide particles are the aggregate and metallic cobalt serves as the matrix. The extremely hard tungsten carbide provides the overall hardness and wear resistance whereas the ductile cobalt (Co), binder phase, will promote the toughness.

Cemented carbide tools render quite useful when employed in rock drilling and metal machining applications where other materials would wear away much faster. They can withstand high stresses, high temperatures and maintain their shape after several working cycles. For cemented carbides are more brittle than other tool materials, they are generally used as small inserts to be assembled on the shank tool made of a more ductile material, generally steel. This renders tools much cheaper, and damaged inserts can be replaced with ease.

High speed steel tools and some rock drilling inserts are sometimes coated in order to improve surface hardness and lubricity, as well to lower the working temperatures. Though the life time is increased, these coated inserts are seldom used in rock drilling applications due to their high price - a diamond coated insert can cost up to four times more than a standard insert – generally they are used in the oil industry where larger depths are to be achieved with one single bit.

Being the dominant material in rock drilling tools [4], the WC-Co cemented carbide will be considered in the following sections.

[fig2] – Cemented carbide tools

2.1 - Production

Tungsten-cobalt carbide is produced thru a sintering process. The WC powder with certain grain size - from 0.5 µm (fine grain) up to 5 µm (extra coarse grain) [1] - is mixed with the desired proportion of cobalt powder and milled together with press agents and milling fluid [2] (other elements like VC, Cr_3C_2 or TaC can also be added as grain growth inhibitors) [6,8]. This slurry mixture will then be spray-dried, i.e. pumped thru an atomiser nozzle producing fine droplets into a drying chamber. Here, a hot nitrogen atmosphere will dry the droplets producing well mixed agglomerates [fig3].

[fig3] - Electron microscope image of the agglomerates resulting from spray drying. Metal and carbide powder with a grain size of 1-3 µm was used, along with PEG (Polyethylene glycol) as press agent. The agglomerates average a 100 µm diameter [6].

A powder compaction press is used to obtain the green bodies (pieces of compacted power held together by the press agent). The agglomerate powder is poured into a vertical die cavity with the required shape, pressed with a punch tool and finally ejected from the cavity.

The green bodies are sintered at 1350- 1500ºC after a preheating cycle at 300-400ºC to burn off the press agents [2]. At the highest temperature the cobalt melts and the WC carbide starts to decompose to tungsten and carbon. During cooling this decomposition reverses leaving only a small amount of dissolved tungsten and carbon that will strengthen the cobalt phase [2]. For some rock drill inserts the whole sintering thermal cycle takes up to 15h. The duration of the cycle is highly dependent on the insert size, geometry and composition.

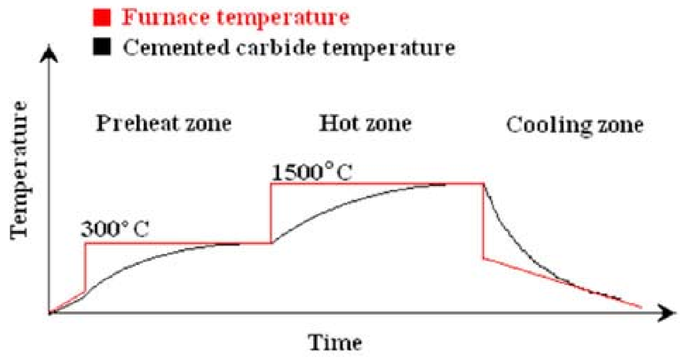

[fig4] - Simplified heating cycle used in cemented carbide sintering

A phenomenon that has to be taken in account during the project of new cemented carbide inserts is the shrinkage i.e. a decrease in dimensions of the compact which occurs during sintering. For example, a green chisel insert with approximate overall dimensions 12.2 x 21.4 x 48.9 mm measures 10.0 x 17.7 x 39.3 mm after sintering. This represents an average 18% of linear shrinking, and approximately 44% of volume reduction. Generally, 17.5% of linear shrinking is the reference value.

[fig5] - Dimensional comparison between green body and cemented carbide insert after sintering

Due to shrinkage, after sintering all the inserts must be ground to the required assembly dimensions. The chisel above mentioned would be ground to the width of 9.9 mm. Tight tolerances can be achieved with standard grinding machines [fig#].

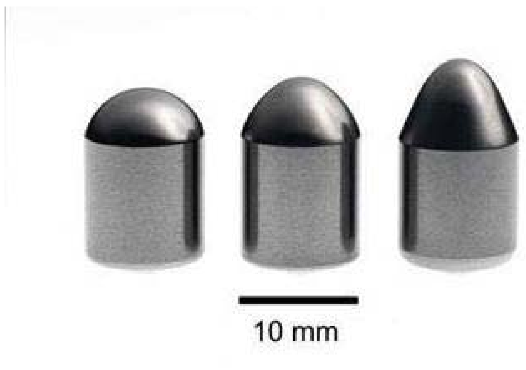

[Fig6] - Cemented carbide inserts ready to be assembled

The quality of the inserts must be frequently evaluated. Thus, sample inserts are frequently collected, measured and weighed. Both the magnetic coercivity and the magnetic saturation are also measured [See section 5.1].

2.2 - Properties

The cemented carbide materials provide a unique combination of hardness and toughness. Their mechanical properties are highly dependent on the relative proportions of cobalt and WC present in its structure. Although many grades for specialised applications lie outside these ranges, in rock drilling applications the current grades range from 6% to 15% of cobalt. These values depend on the ground to be drilled, insert functional role and drilling method. The WC grain size also plays an important role defining the material properties.

In accordance with its non-centrosymmetric crystal structure, the microhardness of WC is highly anisotropic. Thus, it's not surprising that microhardness values measured at arbitrary orientations show a large scatter, and room temperature microhardness values given in the literature have a wide range [3], from 1300HV* up to 2300HV [Fig7] [1]. Until the mid 1960s WC was assumed to be perfectly brittle. There is a lot of evidence, however, that WC shows appreciable plastic deformation. Other essential features of WC are the extremely high elastic modulus, around from 400GPa to 650GPa [1], and its high thermal conductivity.

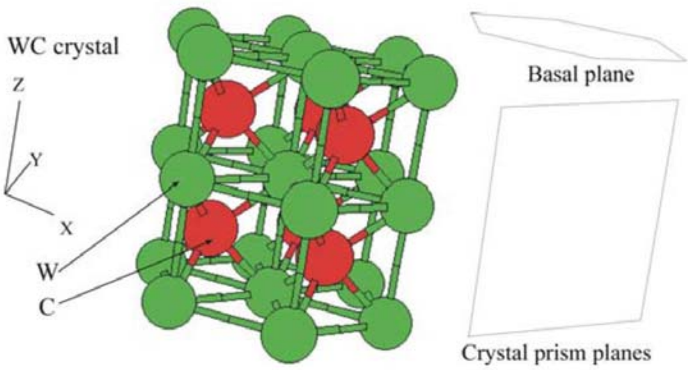

[fig7] - The non-centrosymmetric hexagonal WC crystal structure.Basal planes with 2300 HV and crystal prism plans with 1300 HV.

Cobalt is used nearly exclusively in cemented carbide production (more than 95%) because of its outstanding wetting and adhesion as well as to its advantageous mechanical properties [3]. The bulk hardness of cobalt is bellow 100 HV, but nanohardness tests have shown that Co-binder close to WC-grains is about four times harder than in the bulk [9]. Not much importance is paid to the Co powder properties for they are lost during milling and liquid-phase sintering and thus do not influence the properties of the binder phase.

* All the hardness values in this thesis refer to HV30, i.e. Vickers hardness test with an indent load of 30kg

The relationship between the different properties and compositions is roughly expressed in the following table [fig8]. Although this table is valid in general, there are some deviations which must be considered. Higher binder content at a given hardness, combined with a lower average WC grain size, does not necessarily mean a higher toughness. In the lower hardness range this relationship doesn't even exist. At the higher range, on the other hand, a higher binder can reduce the carbide contiguity and thus improve the hardness to toughness relationship [6]. It has also been found that ultra fine grained hardmetals produced from nanocarbide powders have much superior toughness, particularly at hardness levels above 1500HV, compared to conventional hardmetals [8].

When you increase:	This is what will happen: Cobalt content	Abrasion resistance	Grain size	Hardness HV	Fracture toughness
Cobalt content		↓		↓	↑
Abrasion resistance	↓		↓	↑	↓
Grain size		↓		↓	↑
Hardness HV	↓	↑	↓		↓
Fracture toughness	↑	↓	↑	↓	

[fig8] - Relationship between the different properties of cemented carbides

The overall hardness of cemented carbides ranges approximately from 700 HV, for a grade with 25% cobalt and 5 µm coarse grain size, up to 2200 HV, for a 5% cobalt grade with submicron WC grain size [1].

Toughness is generally evaluated through the Palmqvist method:

$$W = \frac{P}{L}$$

W = Toughness (N/m)

L = Sum of the crack lengths at the corners of a Vickers hardness indentation (m)

P = Indent load (N)

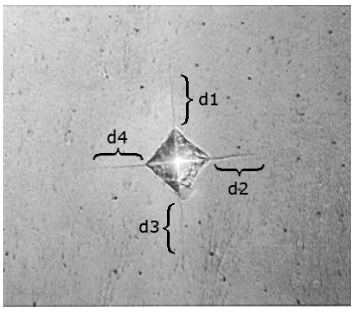

[fig9] - Palmqvist indent with crack lengths

One of the most important properties of cemented carbides is the fracture toughness. It is denoted K_{Ic}, plain-strain fracture toughness, and describes the ability of a material containing a crack to resist fracture. The subscript *Ic* denotes mode I crack opening under a normal tensile stress perpendicular to the crack, since the material can be made thick enough to resist shear (mode II) or tear (mode III).

The following formulae were proposed by different authors and can be used to convert the Palmqvist data into fracture toughness values ($MPa\sqrt{m}$) [6, 8]:

Shetty *et al.*

$$\mathrm{K_{Ic}} = 0.0889\sqrt{\frac{HP}{L}}$$

Where H = Vickers hardness (Nm^{-2})

P = Indent load (N)

L = Total crack length (m)

Peters

$$\mathrm{K_{Ic}} = \frac{0.000319P}{a\sqrt{l}}$$

Where P = Indent load (N)

l = single crack length (m)

a = one half indent diagonal length (m)

Depending on the grades, typical fracture toughness values for cemented carbides lie between 5 $MPa\sqrt{m}$ and 26 $MPa\sqrt{m}$ [1].

3 - Rotary rock drilling

Revolutionized by the appearance of cemented carbides, rock drilling plays an essential role in mining, exploration and water well industries. There are several different applications that need different kinds of drilling equipment and performance. The drilling method has been established for some time, and well proven techniques are seldom replaced by new methods.

Being the world's leader in the manufacturing of rock drilling bits, Atlas Copco Secoroc divided its surface drilling product range in two main groups: rotary percussive and rotary crushing drilling.

Rotary percussive drilling			
Top hammer method: As the name "tophammer" implies, the rock drill is situated on the rig and works on the top of the drill string. The impact energy of the rock drill piston is transmitted to the drill bit in the form of shock waves. Although the method is fast in good rock conditions, the hole depth and straightness are comparatively limited.	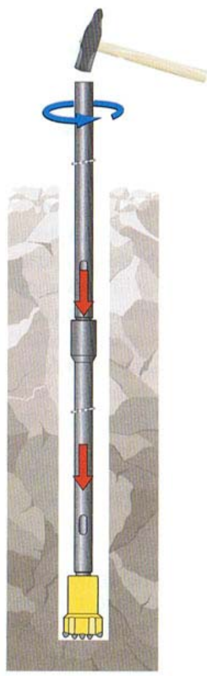 [fig10]	**Down-the-hole method:** The hammer is situated down the hole in direct contact with the drill bit. The hammer piston strikes the drill bit resulting in an efficient transmission of the impact energy and insignificant power losses with the hole depth. The method is widely used for drilling long holes, not only for blasting, but also for water wells, shallow gas and oil wells, and for geo-thermal wells. From an environmental point of view, the noise emissions and vibration from DTH drilling are comparatively low.	 [fig11]

<table>
<tr>
<td rowspan="2">COPROD® system:

The rock drill is situated on the feed beam on the rig and impact energy is imparted from above. Threadless impact rods are stacked inside the threaded drill pipes. The impact rods are used solely to transmit impact energy and feed force, while the drill pipes transmit rotation. COPROD combines the speed of tophammer drilling with the hole straightness of the down-the-hole method.</td>
<td rowspan="2">
[fig12]</td>
<td colspan="2"><u>Rotary crushing drilling</u></td>
</tr>
<tr>
<td>Rotation is provided by a hydraulic or electric motor driven gearbox, called rotary head that moves up and down the tower via a feed system, generating the pulldown required to give sufficient weight on the bit. Flushing of drill cuttings between the wall of the hole and the drill rods is normally made with compressed air.</td>
<td>

[fig13]</td>
</tr>
</table>

3.1 - Rotary crushing drilling

The prime difference from other drilling methods is the absence of percussion. Rotary cutting using fixed type claw or drag bits, is mainly used for soft rock which is cut by shearing. Rotary crushing uses tricone bits relying on crushing and spalling the rock. This is accomplished by transferring downforce, known as pulldown, to the bit while rotating in order to drive the teeth into the hole bottom as the three cones rotate around their respective axis. The softer the rock, the higher the rotation speed. The drill rigs need to be heavy in order to avoid the lifting of the jacks, which means they are less flexible and not very well suited for drilling at different angles.

Generally, drilling bellow 152 mm is best accomplished by percussive drilling unless prevailing rock conditions are suited for rotary cutting. Rotary crushing is the prime choice for large diameter holes, above 254 mm in open pit mining, overburden stripping at coal mines, and deep well drilling.

[fig14] – Rotary crushing drill rigs

Flushing of the drill cuttings between the wall of the drill hole and the drill rods is normally made with compressed air.

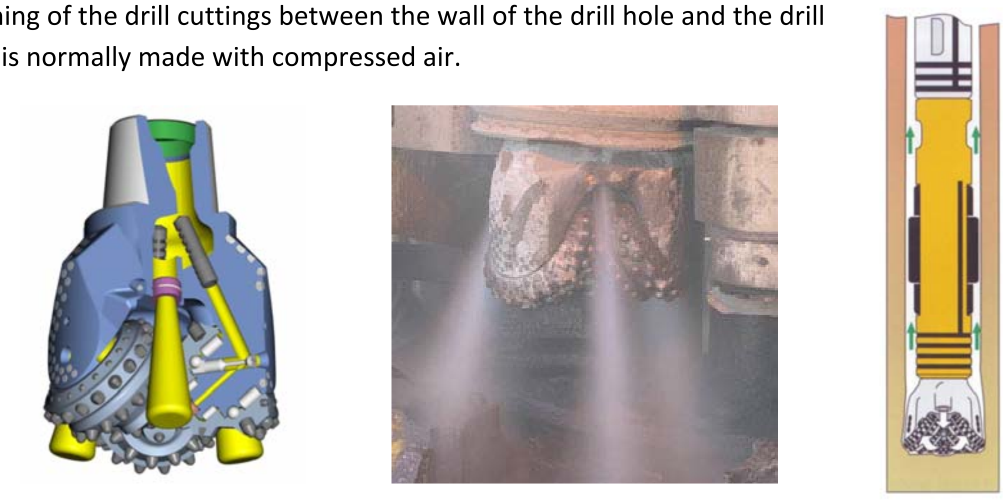

[fig15] - Air pathway through the nozzles and lugs; Flushing of the drill cuttings

[fig16] – Rotary bit ready to be used

The tricone drill bits are composed of three cones. The cones make up the cutting elements of the rock bit and are comprised of the following:

WC carbide inserts – which are pressed into the softer steel material with interference fit to hold them in place;

Cone thrust button – made of a wear resistant material used to take axial loads;

Outer cone shell – Insert's bores and cone grooves;

Cone bore – internal ball and roller bearing races;

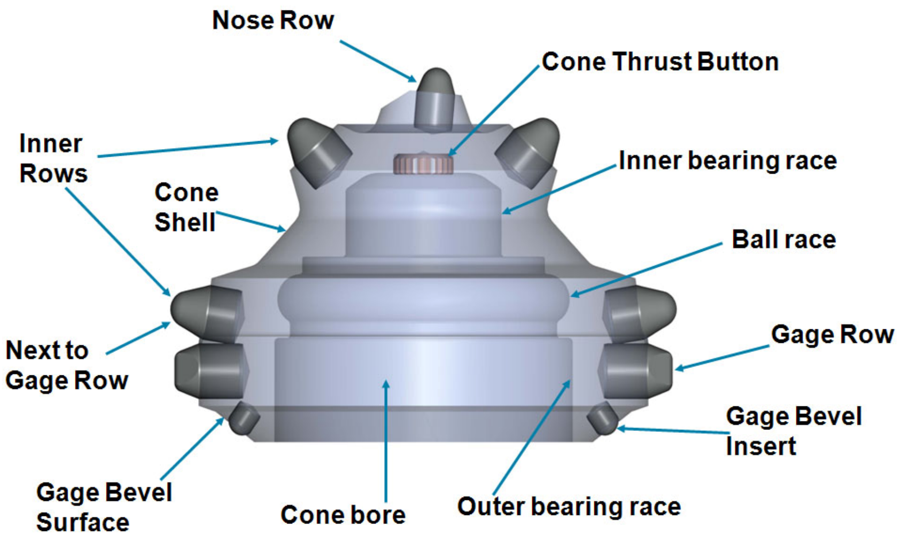

[fig17] – Rotary bit cone with inserts

The lugs are coupled in three by 120º and welded together to form the bit body and the pin connection. The bearing inner races and the nozzle holders are machined directly in the lugs. The shirttail protection inserts prevent the side wear caused by the rock cuttings flushed from the bottom of the hole.

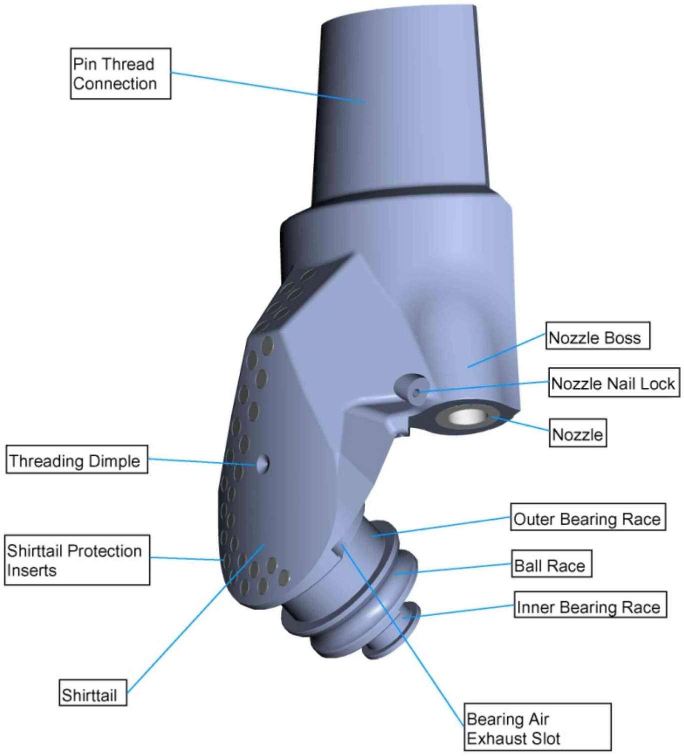

[fig18] – Rotary bit lug

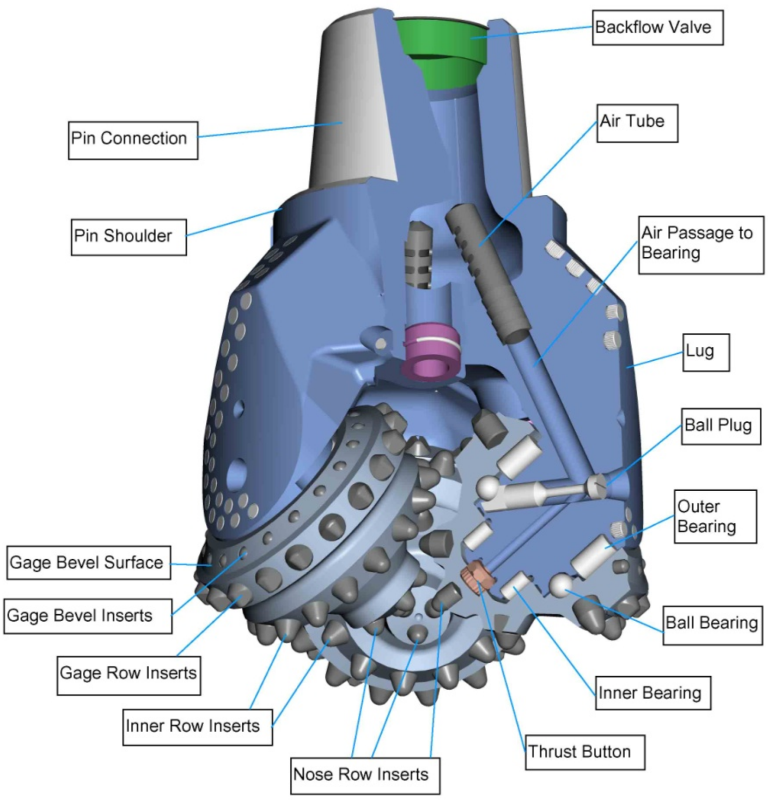

[fig19] – Cut view of complete rotary bit

4 - Rock drill wear and deterioration mechanisms

The wear and deterioration of cemented carbides is an intricate subject of the utmost importance that has been actively investigated in the last few years. Many authors have contributed with considerable developments in this field. Though, given its complexity, there are still many questions remaining to be solved.

For it's not part of the main theme of this work, this subject will only be briefly discussed.

The first stage of the cemented carbide wear is the surface deterioration. It can be caused by several different mechanisms, found in the following groups [1]:

- Rock cover formation, rock intermixing and penetration – small particles of rock penetrate the insert structure creating both a continuous outer layer of mixed material as well as deep channels filled with rock.

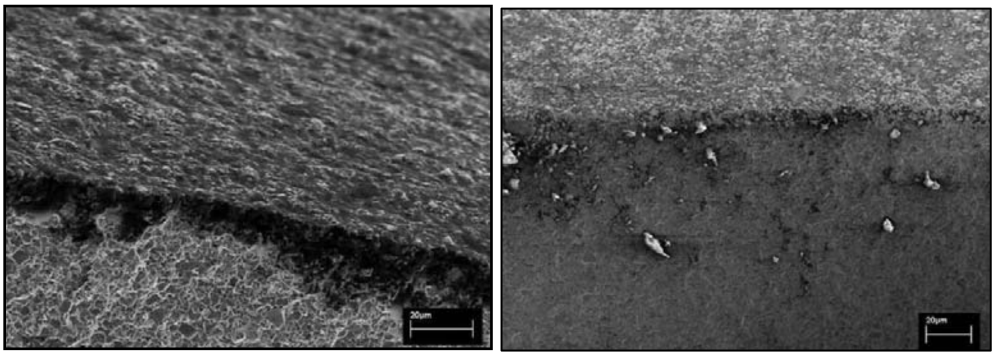

[fig20] – Mixed surface layer and rock penetration in the cemented carbide structure

- Embrittlement and degradation of the binder phase – the presence of cyclic stress, by shifting temperature or load, will lead to material fatigue. The subsequent structural changes will promote the appearance of cracks, and thus surface deterioration.

- Composite-scale crack formation – a thermal wear mechanism. It compasses the known "Reptile skin formation". This is a particular deterioration mechanism found when drilling soft rock types like the magnetite. To avoid catastrophic cracks, the drills inserts have to be regularly ground down to the bottom of the valleys.

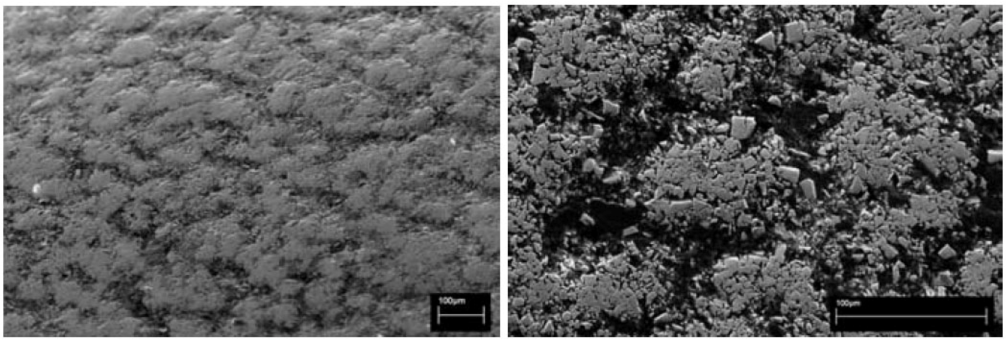

[fig21] – Reptile skin formation found in cemented carbide insert used to drill magnetite

- Cracking of single WC grains – plastic deformation and fragmentation of carbide grains can happen whilst drilling hard rock types, especially under abrasive conditions.

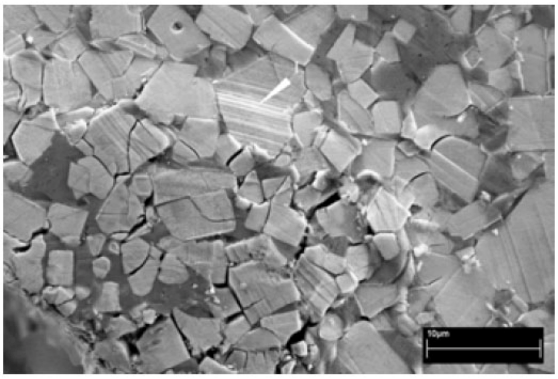

[fig22] – Cemented carbide showing plastically deformed WC grains

- Oxidation and corrosion of WC grains

These deterioration mechanisms will led to the detachment of cemented carbide particles from the insert surface. Sometimes there's catastrophic failure of the inserts without previous deterioration. This can be caused by the presence of some hard material in the hole bottom. This hard material, generally coming from broken defective inserts, will hit the drill inserts and cause them to break. These broken insert particles can lead to the destruction of the whole drill bit. For this reason the production of cemented carbide inserts has to undergo tight quality control.

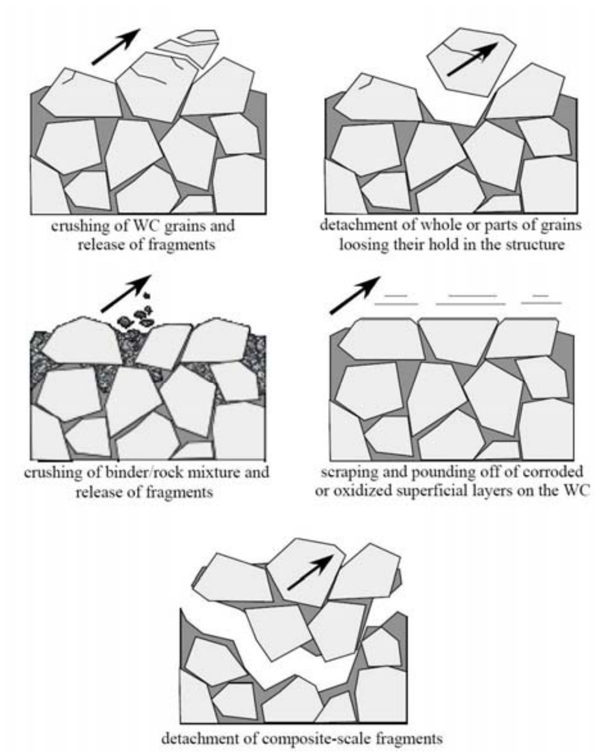

[fig23] – Detachment mechanisms in cemented carbide inserts

5 - Cemented carbide testing

The evaluation of cemented carbides and the comparison of different grades are important matters that have to be taken in account whilst producing and developing the drill inserts. The testing methods were divided into four different groups according to their complexity and proximity to real drilling conditions.

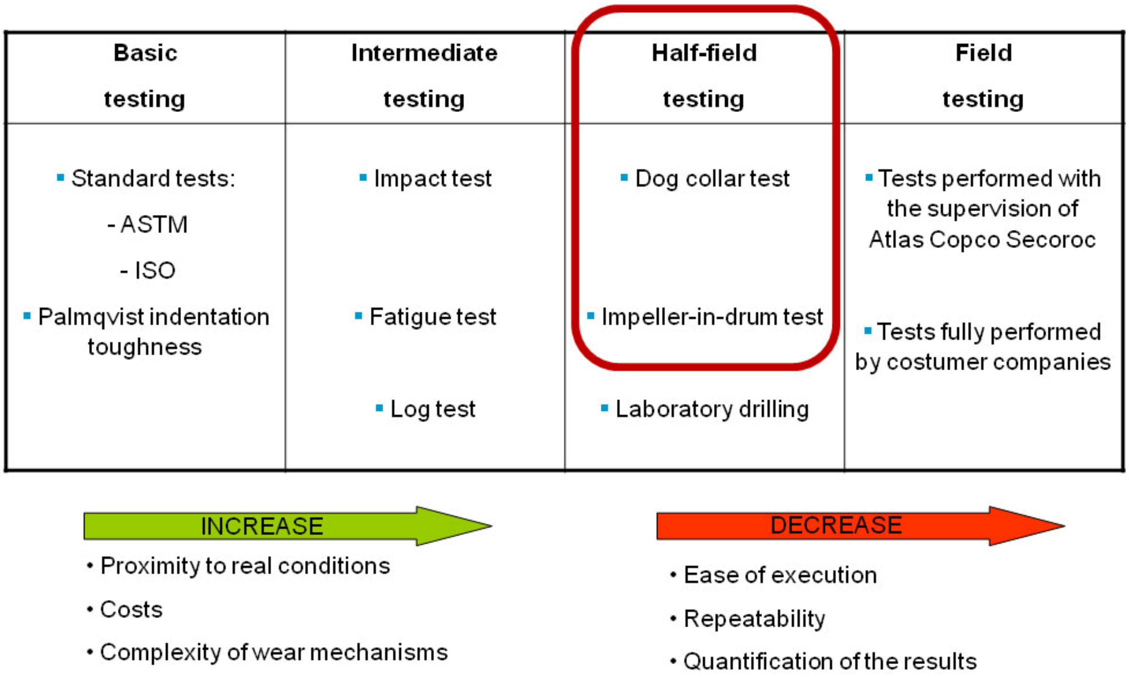

[fig24] – Cemented carbide testing chart

5.1 - Basic testing

Standard tests

There are several organizations developing and publishing standardized procedures for materials testing. ASTM International, originally known as American Society for Testing and Materials, is one of the best known organizations of this kind that offers a wide range of standards related to the cemented carbide testing. Another highly respect organization is the International Organization for Standardization – ISO. For these are probably the best known worldwide organizations, their publications are followed by most of the cemented carbide producers. The most commonly measured parameters to assess quality and define application areas are described bellow:

Porosity - Residual Porosity is determined by visually examining the polished surface of a sintered sample at 100X or 200X magnification. Ratings for “A” type porosity (pores less than 10 microns in diameter), “B” type porosity (pores larger than 10 microns in diameter), and “C” type porosity (carbon inclusions) are determined by comparing the size and frequencies of each pore type in the sample with those in standard photographs. Each standard photograph is associated with a numerical rating that is used to represent the porosity levels in the sample. In general, edge strength and toughness decrease as the level of residual porosity increases. At high levels of porosity, the wear resistance of the product may also be adversely affected.

ASTM B276:05e1 - Standard Test Method for Apparent Porosity in Cemented Carbides

ISO 4505:1978 – Hardmetals - Metallographic determination of porosity and uncombined carbon

Magnetic saturation - Magnetic Saturation is the degree to which the metal binder in a cemented carbide is saturated with carbon. It is most useful for materials having a cobalt binder. For a known cobalt content magnetic saturation values indicate how much carbon the cemented carbide contains – from unacceptably low values that indicate the presence of an undesirable carbon-deficient phase (known as eta phase) to unacceptably high values indicating the presence of free carbon (carbon “porosity”) in the product. Magnetic saturation is sometimes used as an indicator of relative strength among lots of a specific grade.

ASTM B886:03(2008) - Standard Test Method for Determination of Magnetic Saturation (Ms) of Cemented Carbides

Magnetic Coercivity - Coercive Force is the strength of the magnetic field required to demagnetize a fully magnetized cemented carbide sample. Coercive force is typically measured in *oersteds* (Oe). The coercive force measurement depends on many factors including composition, sintered grain size distribution, residual porosity levels, and others. It is sometimes used as an alternative indication of hardness, but is best interpreted in combination with other properties as a measure of overall grade uniformity. The mean free path, which is a measure of the average thickness of cobalt between the WC grains, can be also indirectly determined by measuring the magnetic coercivity force [1].

ASTM B887:03 - Standard Test Method for Determination of Coercivity (Hcs) of Cemented Carbides

ISO 3326:1975 - Hardmetals - Determination of (the magnetization) coercivity

Hardness - Hardness is the resistance of a cemented carbide to penetration by a diamond indenter under a specific load. It is measured on the Rockwell A (Ra) scale in the US and on the Vickers (HV10 or HV30) scale in Europe and elsewhere. Hardness is primarily a function of composition and grain size with higher binder metal contents and coarser tungsten carbide grain sizes producing lower hardness values. Conversely, low binder contents and fine grain sizes produce high hardness values. Hardness is directly related to abrasive wear resistance.

Rockwell Hardness

ASTM B294:92(2006) - Standard Test Method for Hardness Testing of Cemented Carbides

ISO 3738-1:1982 - Hardmetals - Rockwell hardness test (scale A) - Part 1: Test method

ISO 3738-2:1988 - Hardmetals - Rockwell hardness test (scale A) - Part 2: Preparation and calibration of standard test blocks

Vickers Hardness

ISO 3878:1983 - Hardmetals - Vickers hardness test

ASTM C1327:08 - Standard Test Method for Vickers Indentation Hardness of Advanced Ceramics

Transverse Rupture Strength - Transverse Rupture Strength (TRS) is a measure of the tensile strength of a cemented carbide in a three point bending test performed on standard rectangular bars. It is reported in units of pounds per square inch (psi), or in Newtons per square millimeter (N/mm^2). TRS is perhaps the best measure of the relative utility of individual production batches since it surveys a reasonable volume of material and will detect low levels of critical internal defects. Products having relatively high TRS values are generally applied where shock, impact, or failure by breakage are factors

ASTM B406:96(2005) - Standard Test Method for Transverse Rupture Strength of Cemented Carbides

ISO 3327:1982 - Hardmetals - Determination of transverse rupture strength

<u>Density</u> - Density is the weight per unit volume of a cemented carbide measured in grams per cubic centimeter (g/cm^3). It is essentially the weighted average of the densities of all of the components contained in the product and is therefore a check on its composition.

ASTM B311:93(2002)e1 - Test Method for Density Determination for Powder Metallurgy (P/M) Materials Containing Less Than Two Percent Porosity

ISO 3369:1975 - Impermeable sintered metal materials and hardmetals - Determination of density

<u>Grain size</u> – The average grain size is determined by visually examining photomicrographs of the cemented carbide surface. It depends merely on the chosen WC powder and has great influence on the hardness and toughness. The introduction of the spray conversion process for the production of WC-Co powders in the size range 20-30nm has resulted in the development of “nanocrystalline” hardmetals whose properties have considerably improved in comparison to those similar coarse grained materials.

ISO 4499-1 - Hardmetals - Metallographic determination of microstructure - Part 1: Photomicrographs and description

ISO 4499-2 - Hardmetals - Metallographic determination of microstructure -- Part 2: Measurement of WC grain size

Non-standardized tests

<u>Palmqvist indentation toughness</u> – refer to section 2.2

5.2 - Intermediate testing

5.2.1 - Impact test

In this test the basic principle is to drop the test specimen against a fixed object or surface. The impact energy is then measured, and the specimen is dropped again a given number of times, or until it breaks. There are commercially available rigs designed to perform these tests. They can monitor and control several parameters like the impact energy, impact velocity, number of impacts until failure, temperature, etc. These machines are distributed with specific software for data handling. This renders the acquisition of practical results simple and expeditious. Though, these machines are generally expensive.

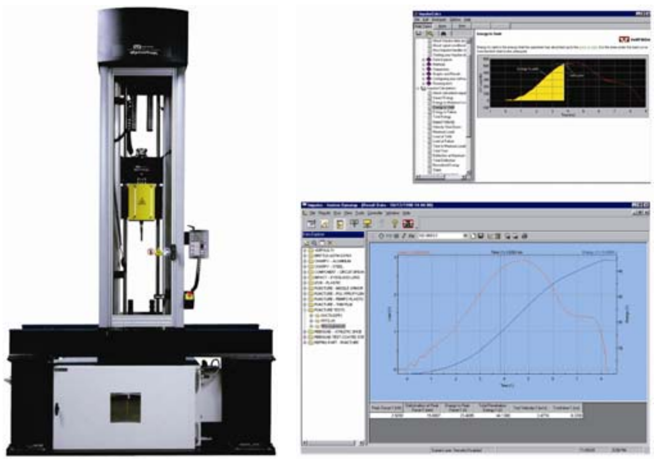

[fig25] - Impact test machine with controlling and data acquisition/handling system

5.2.2 - Fatigue test

Here, fatigue load is induced in the test specimens. Like the previous, there are commercially available solutions ready to use. They rely generally on a hydraulic loading system and precise load cells specifically designed for this purpose. Yet again, like most of the material testing equipment of this sort, these test rigs are generally expensive.

[fig26] - Fatigue test machine with controlling and data analysis software. Specifically designed load cell

5.2.3 - Log test

This test is currently being performed by several hardmetal producers. For there is no commercially available solution, all the test rigs are built in-house. This is an abrasion test and the basic principle is to press a hardmetal test specimen against a rotating stone log placed in a horizontal lathe. The specimen then is moved along the log surface for some time, and finally removed and analysed.

[fig27] - Representation of horizontal lathe performing the log test

In order to prevent excessive rubbing, full inserts cannot be used. The smaller test specimens are generally obtained cutting the insert three times in the longitudinal direction.

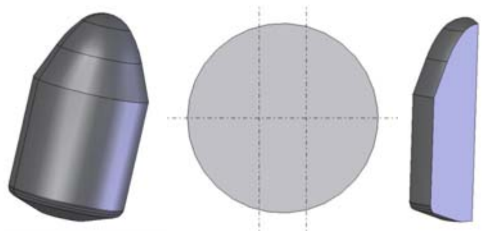

[fig28] - Full insert perspective view, top view with cutting lines and final test specimen

In order to prevent the log from breaking, the tests have to be stopped when a specific minimum diameter is reached. A 150 mm wide log is worn down solely down to 85 mm, i.e. only 45% of the total rock volume is actually used.

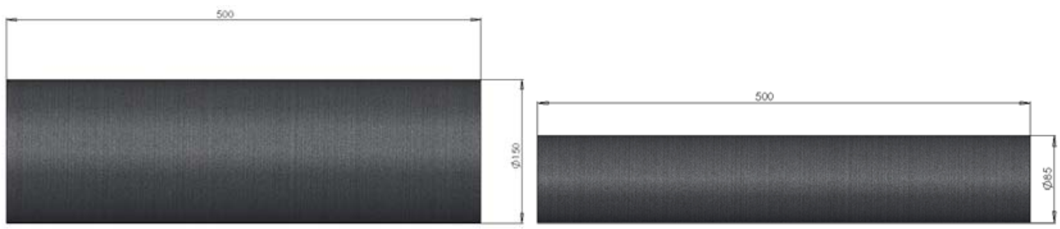

[fig29] - Initial and worn log

Advantages:	**Disadvantages:**
- Low maintenance and purchase costs	- Log shaped rock required
- Simple process	- Only 43% of the rock volume is used
- Quantitative and qualitative results	- Laborious process to obtain test specimens
	- Test specimens different from production inserts

[fig30] - Advantages and disadvantages of the log test

5.3 - Half-field testing

5.3.1 - Dog-collar test rig design and specifications

5.3.1.1 - Abstract

This test is used to simulate rotary crushing drilling. It is an impact-abrasive wear test and probably the best approximation method to the real conditions. The test rig is a rather complex mechanism and is not commercially available. Despite this fact there are several hardmetals producers performing and investing in this test.

Basically the cemented carbide inserts are hot fitted around a steel disc in a way that resembles a dog-collar. This collar in then pressed against, and moved along a rotating stone with a flat surface. The friction will force the collar to rotate around its axis [fig31].

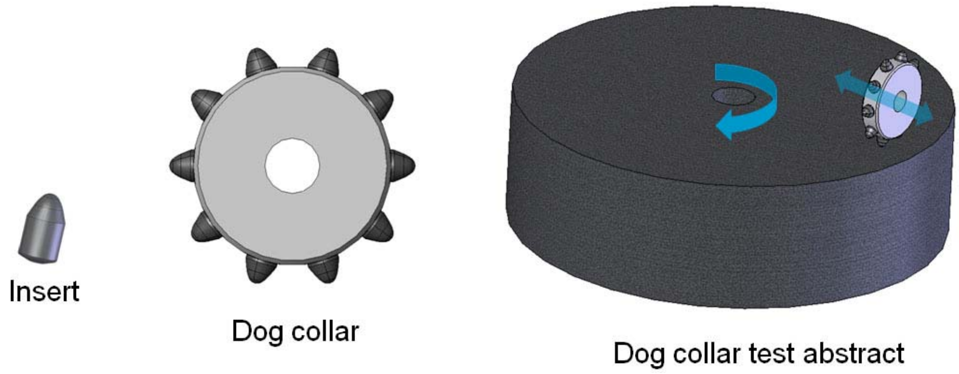

[fig31] – Dog-collar test elements

5.3.1.2 - State-of-art

Most of the companies performing this test use a modified vertical turret lathe. They simply build a dog-collar holder and assemble it in the modified turret. The position of the tool and the rotational speed are the only two variables to be controlled. For this test requires a large volume of rock to be handled, the lathes are rather bulky and heavy [fig32].

[fig32] – Vertical lathe with rock and silhouette as dimensional reference

[fig33] – Dog-collar test being performed. The tracking in the rock surface is clearly visible.

5.3.1.3 - Requirements

- Simulate real conditions as close as possible:

- A maximum of 500kg of load per insert. Though this value is seldom reached and not recommended in practical drilling, the test rig should reach it in order to evaluate future grades with improved qualities. A maximum of 175Kg per mm of bit diameter is the goal to be reached as rule of thumb for the maximum pull down force per bit. 140Kg/mm is the maximum recommended value.

- 43 insert hits per second – yet again, this is a maximum value. It corresponds to an average bit rotational speed of 150 RPM.

- Cone shift of two degrees – The tricone bits are produced with a cone shift of approximately 2 degrees from its axis of rotation. This is done in order to promote rubbing between the bit and the rock, thus leading to abrasive wear.

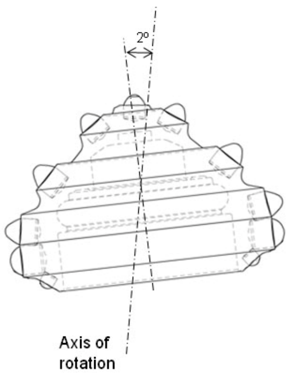

[fig34] – Cone shift around its centre of gravity. This deviation from the axis of rotation will promote the abrasive wear.

- Compact overall dimensions

- Ease of controlling

- Simple and reliable construction
- Meet safety criteria
- Low maintenance
- Low purchase and operation costs
- Repeatability of test conditions
- Flexibility to simulate different conditions

5.3.1.4 - First solutions – Vertical turret lathe

The first solution to be taken in account was to do the same thing as the competitors, i.e. using a modified vertical lathe. After a market survey, some problems arose:

- The new lathes are too expensive: all the new lathes cost more than the budget for the whole project, i.e. 50.000€. Thus, the lathe would have to be bought in a second hand state which would certainly void the warranty;
- Lathes are high precision equipment: for precision is not a requirement of this test rig, a considerable expense would have to be paid for a useless feature;
- Second hand fully-functional lathes are still expensive – the price tag for these second hand lathes goes from 40.000€ (for a non-functional old lathe), up to 330.000€ (for fully-functional lathe with control system);

[fig35] – Second hand vertical turret lathes found at www.machinestock.com

- The acme threads cannot take much load: the tool holder is guided using acme threads. These threads are good for high precision displacements but they are not designed to take high loads.

[fig36] – Acme thread used to guide and move the tool holder in vertical lathes

- Bigger threads require bigger lathe: in order to take the required load, the guiding acme threads would have to be bigger. These oversized threads can only be found in big lathes;
- No need for turret, it would have to be removed: most of the lathes come with a turret for quick tool exchange. For it is not necessary, it would have to be removed or modified;
- Control system would have to be added: for fully functional lathes with control system are too expensive, a control system would have to be developed. This couldn't be done without considerable work and the costs would be probably high.
- Position controlling and not load control: one of the main issues of this solution is that the lathes control the tool position and not the load on the tool. This fact would surely increase the gap between the real and the simulated drilling conditions.

Although most of these issues could be solved, they would certainly increase the overall expenses above the budget.

5.3.1.5 - First solutions – Column shaping machine

[fig37] – Column shaping machine

Another solution that was also taken in account was to use a column shaping machine. These commercially available machines are quite common in the stone industry. They are used to shape circular columns. There of some advantages worth of notice, namely: the tool holder has the two required degrees of freedom, and the turntable is designed to handle stone. Given their low precision and simple construction these machines are also available for a low price (approximately 4.000€). But, like in the previous solution, some problems came to discussion:

- The tool holder is not designed to take high loads: it would have to be modified;
- Feeble structure to take a high load on the tool: the frame design would not permit high loads on the tool holder, it would have to be reinforced;
- Position controlling and not load control: as in the previous solution this would be one of the main issues;
- The guiding rails are designed to hold solely the cutting tool, an angle grinder. Therefore, this guiding system would have to be substituted or reinforced;

Due to the fact that all the needed modifications would probably raise safety issues, the development of this solution was not resumed.

5.3.1.6 - In-house solution

Finally, the idea of projecting the whole test rig came to mind. It could be designed and assembled in-house and all the components would have to be chosen from different suppliers. Some parts would have to be machined and a considerable amount of time would have to be spent. Despite these facts this was feasible project that would meet all the requirements and probably keep the overall expenses under the budget. After several different proposals a final sketch was considered to be the simplest and easiest solution [fig38].

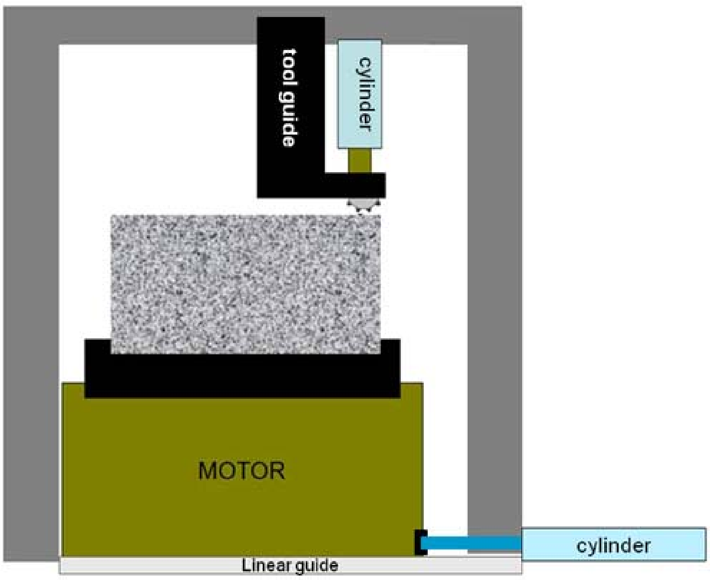

[fig38] – Dog-collar test rig final sketch

In this sketch we can see the main components and the basic mechanism. The rock would be placed in the rotary table. This table would be placed over a linear guide and moved to side with a pneumatic or hydraulic cylinder. The tool would be vertically moved with another cylinder, and held in the right position with a tool guide.

The final test rig is shown in the next figure. In the next sections all the different components will be discussed.

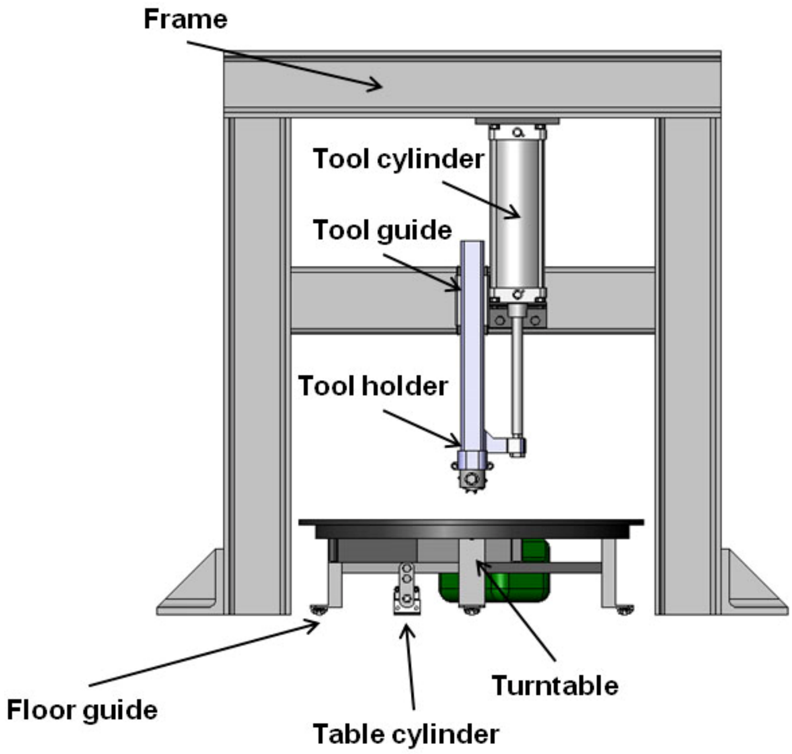

[fig39] – Final test rig with all the different components indicated

5.3.1.7 - Frame

The frame would be made of structural steel. Given its simplicity, robustness and low weight, I-beams could be used. The structure would be welded together and bolted to the ground. A standard I-beam with the following dimensions would be used:

Standard wide flange I-beam W10x68 (10” wide, 68Lbs/inch)

Section: 254 x 254 mm, web: 11.94mm, flange: 19.56mm

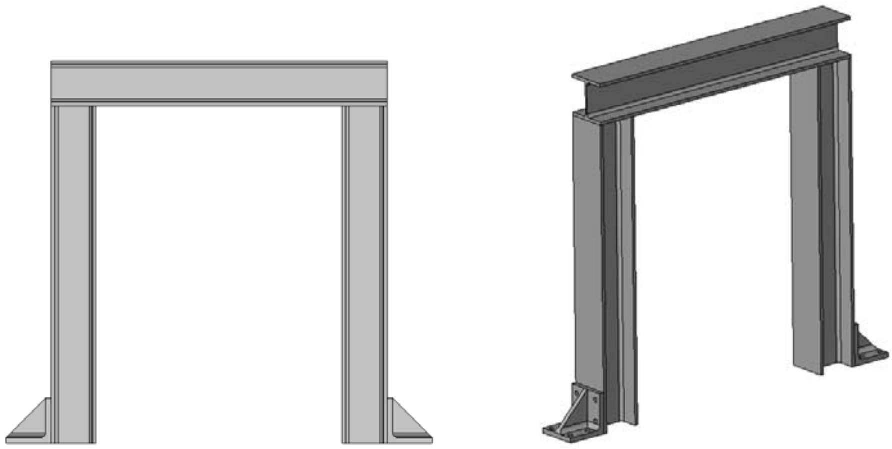

[fig40] – Test rig frame

5.3.1.8 - Turntable

For the rock rotational movement the table would have to meet the following requirements:

- Built-in rotational speed control system;
- High loading capacity;
- Possibility of taking non-centred loading;
- Rotational speed over 25 RPM;
- Robustness for rock handling;
- Low maintenance over time;

The first idea was to use rotary table like the ones used in the vertical lathes. These tables can easily take non-centred load and reach high velocities. Although, given their high precision, these tables are rather expensive. For most of them are hydraulically actuated, they seldom come with a speed control system. For these reasons, this idea was abandoned.

The second idea was to buy a turntable. For no precision is required, these are generally less expensive and can be bought with the control system. The main problem was that most of the turntables are designed to take exclusively centred load, and when they're not, the load capacity is rather small.[fig41]

[fig41] – Rotary table hydraulically actuated and turntable for centred loading.

The final choice was to use a depalletizer – a turntable used in uncoiling applications [fig42]. With a table-top diameter of 1320 mm it can reach 28 rpm. This is a considerable value taking the maximum load into account - approximately 5440 Kg.

[fig42] - Depalletizer – a turntable used in uncoiling applications

For the rotating table-top is supported in its periphery by four ball bearings, this table can take non-centred load without any particular problem. Instead of the central axel the table-top is guided with two side rollers and a clever torque transfer system. This leverage-based system will increase the friction between the driving well and the table-top with the increase of the resistant torque [fig43].

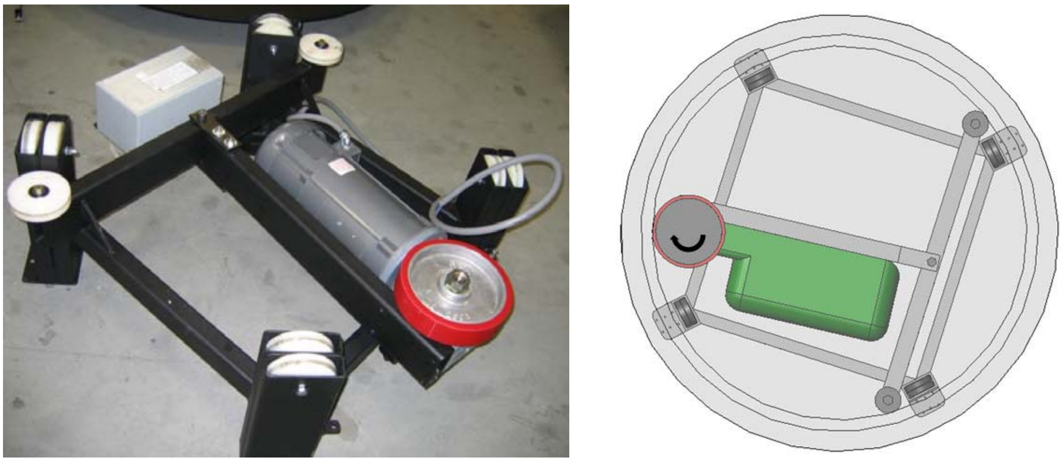

[fig43] – On the left picture we can see the turntable frame with the four support points and two guiding rollers. The driving wheel is connected to the motor and its outer surface is made of (red) rubber in order to promote friction. The picture on the right shows the turntable model top view with the motor (green) placed in a leverage rod that, due to rotation, will push the driving wheel against the table inner driving side.

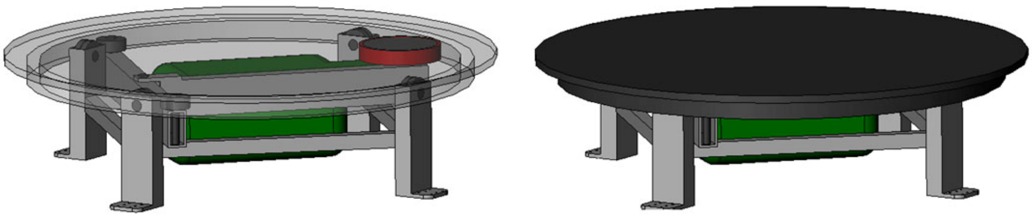

[fig44] – Turntable model side view

These tables are reasonably cheap, and the producer (http://www.norwalkinnovation.com/) claims they're maintenance free. They are also quite compact (400 mm of height), and they come with built-in velocity control system. The power output of 1.5KW would be enough to overcome the rock inertia and the dog-collar friction against the rock.

5.3.1.9 - Size of the rock

The rock samples used to perform this test have to be dimensioned as function of the table loading capacity. Thus, for a maximum tool load of 1000 Kg, the maximum advisable rock weight would be: 5440 – 1000 = 4440 Kg. For an average rock density of 14.4 g/cm^3 (density of granite) the overall dimensions would have to within the graphic area [fig45].

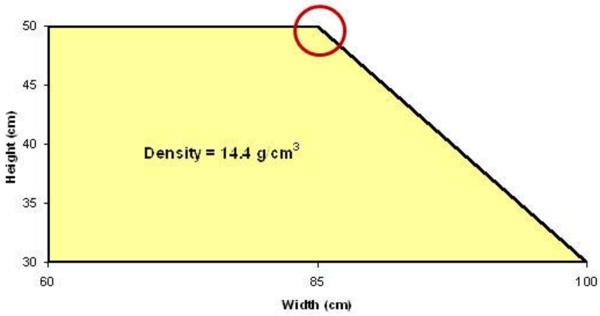

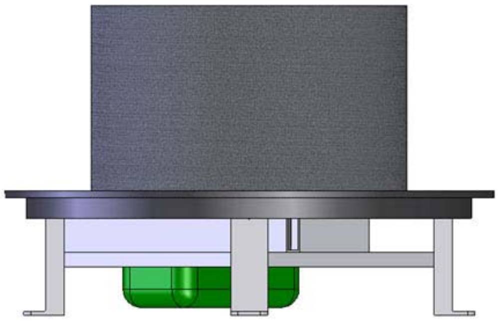

[fig45] – The rock dimensions would have to be within the yellow graphic area. On the left there's a side view of the turntable with the rock (with the dimensions indicated by the red circle) on the top.

5.3.1.10 - Table cylinder

A pneumatic solution was chosen for the turntable transverse movement. For no precision, high velocity or high forces are required, a pneumatic cylinder could suit this application. The seesaw movement could be controlled by a simple pneumatic system without the need of electric components. There is a compressed air network in the laboratory where the test rig would be placed.

It would have to be a double-acting symmetric cylinder in order to have the same piston velocity in both directions. And given this fact, it would have to be compact in order to fit under the turntable.

[fig46] – Double-acting symmetric cylinder

The first step was to do the cylinder dimensioning as function of the required forces:

1 - Maximum weight to be moved:

The maximum turntable load is 5440 kg. The turntable weight is approximately 420 kg.

6.000 kg will be the considered the total maximum weight (W)

2 - Maximum friction load:

According to the producer, the friction coefficient of the ball rail system is approximately 0.002 to 0.003, thus:

F_F = 0.003 x 6000 x 10 = 180 N

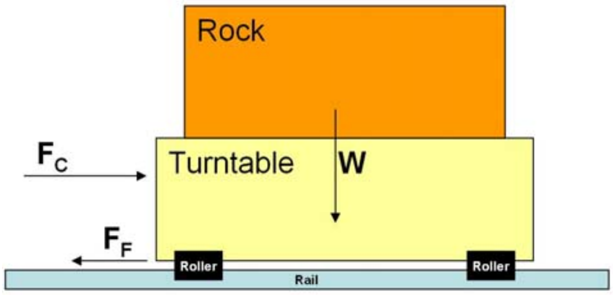

[fig47] – Pneumatic cylinder dimensioning

3 – Given its dimensions compatible with the turntable size, the 80 mm piston cylinder was considered:

Cylinder force, F_C:

Network pressure = 5.5 bar ≈ 5.5 x 10^5 Pa

Piston area ≈ 0,005 m^2 ; Piston rod area ≈ 0,0005 m^2

F_C = (0,005 – 0,0005) x 5.5 x 10^5 ≈ 25.000 N

Considering an efficiency of 80% (usual value for pneumatic cylinders)

F_C ≈ 20.000N

Applying Newton’s law, with A = system acceleration:

$F_C – F_F$ = W x A

A ≈ 3, 3 m/s^2

Theoretically, starting from a rest position this acceleration will allow the table to move 50 cm in approximately 0.5 seconds. Although this value would not be achieved (due to the air supply flow, tool friction, etc) in practical conditions, this value is high enough to confirm the cylinder choice.

The pneumatic system would use a 4/2 way pneumatically actuated valve to control the piston movement, commanded by two 3/2 way valves mechanically actuated that would be placed in both ends of travel, thus making the cylinder return when it reaches those points [see attachment #2].

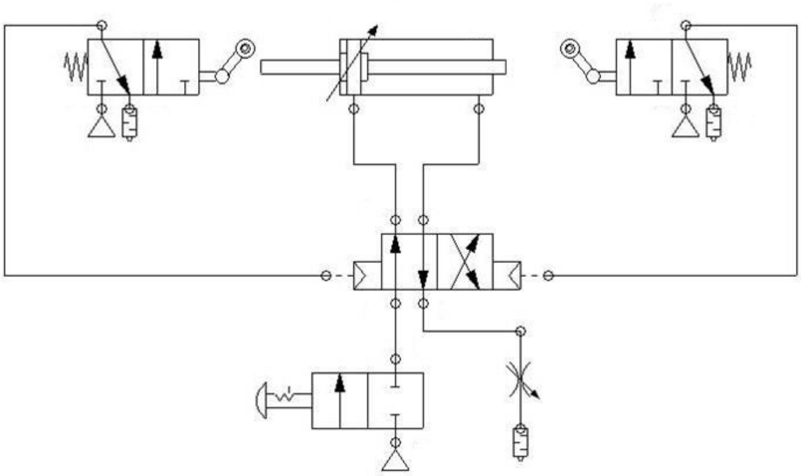

[fig48] – Pneumatic diagram for the turntable seesaw acting system

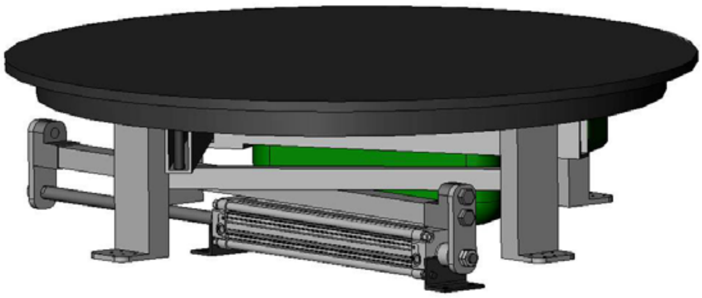

[fig49] – Table with assembled cylinder

5.3.1.11 - Floor guiding system

For the floor guiding system the choice was to use *Bosch Rexroth* linear motion technologies. Bosch offers a comprehensive range of guide rails and runner blocks, virtually suitable for any task involving linear motion and high loads.

Given the required loading capacity, the *Ball Rail System* was chosen. It uses a continuous row of steel balls on both sides of the runner blocks. These are placed with preload in the guiding rail, and the strip holders are assembled on both edges.

[fig50] – Ball rail system, the ball rows are visible on both sides

The chosen runner blocks and rails were:

Runner block - Flanged normal standard width FNS:

- Size 20; Accuracy class N; 24400 N normal loading capacity; C1 Preload class

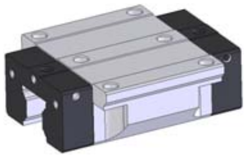

[fig51] – Runner block

Standard guide rails for mounting from above with rail seal and strip holder

- Size 20; Accuracy class N; Length: two rails with 1076 mm and one with 2250 mm

[fig52] – Guide rail with strip holders

5.3.1.12 - Tool guiding system

For the tool guiding system the choice was to use *Bosch Rexroth* technology once more. The *Roller Rail System* is guiding system that, instead of steel balls, uses cylindrical rollers. This enables the maximum advisable loads in the runner block to be much higher.

The size choice would have to be done as function of the maximum torque in the fixing point. Here, the runner block would be fastened to the frame, and the rail connected to the moving tool.

While performing this test the dog-collar rotates over the rock surface. In order to promote abrasive wear there can be a shift in the collar preventing its axis of rotation from being aligned with the rock centre. The friction between the dog-collar and the rock surface won't probably reach such a high value, though, for security reasons the considered friction coefficient will be = 1.

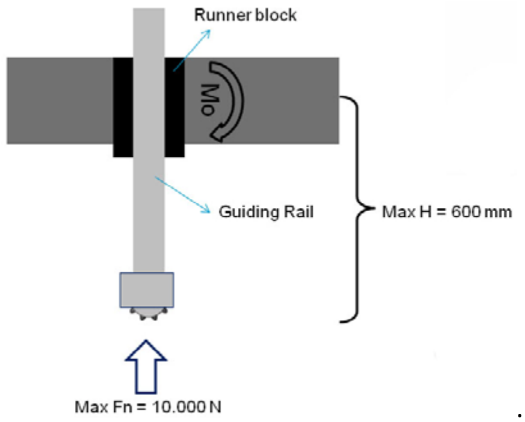

Mo = 1 x 10000 x 0.6 = 6000 Nm

For a runner block size 65, the maximum permitted Mo is 15.760Nm [fig53]. This value is considerably higher than the maximum required torque, thus confirming this choice.

Size	Load capacities (N)		Moment loads (Nm)			
	C	C_0	M_t	M_{t0}	M_L	M_{L0}
65	265 500	525 600	9 410	18 630	7 960	15 760

[fig53] – Maximum advisable loads and torques for the roller runner blocks given in the manufacturer catalogue

5.3.1.13 - Tool cylinder

The tool cylinder [fig54] has to reach the maximum required load of 1000kg. This value can be easily obtained with a pneumatic cylinder connected to the air network available. Considering a maximum air pressure of 5.5 bar, and an efficiency of 80%, with a piston diameter of 200 mm the load would be approximately 1380 Kg.

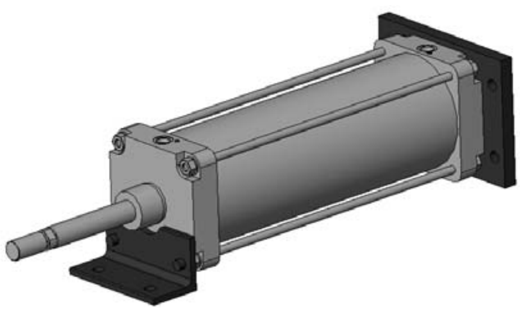

[fig54] – Tool cylinder

Although this value is above the maximum required, the choice of using the 200 mm piston cylinder was made in order to avoid insufficient loading due to air network pressure drops.

The tool displacement and load could be controlled with a simple pneumatic system [fig55]. A pressure control valve with manometer would allow the controller to determine the cylinder force, and a directional valve would control the movement direction [see attachment #1].

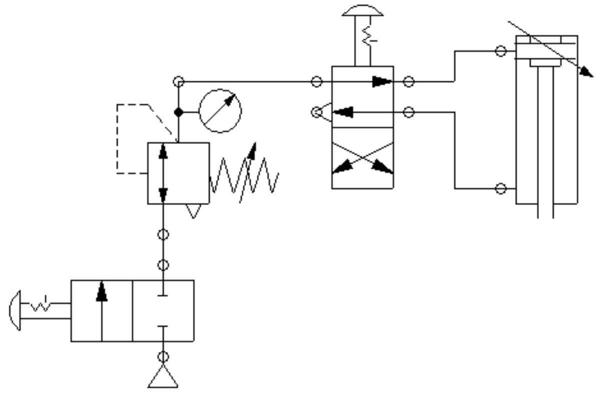

Pressure (bar)	Load (Kg)
2	500
3	750
4	1000

[fig55] - Pneumatic diagram for the tool acting system. Table relating manometer pressure and tool load.

5.3.1.14 – Dog-collar

The dog-collar would have 10 inserts. At 28 Rpm (rotational speed of the table), this will lead to a maximum insert hit frequency of 41. Although this value is under the required, 43, the difference is acceptable without considerable deviation from the real conditions. The number of insert per dog-collar could be reduced in order to decrease the radius, thus increasing the hit frequency.

The inserts could be hot fitted around the steel prop disc, or, alternatively the disc could be composed of two halves that would be bolted together, thus holding the inserts. This last solution would simplify the process of exchanging the inserts, though it wouldn't be as robust as the first.

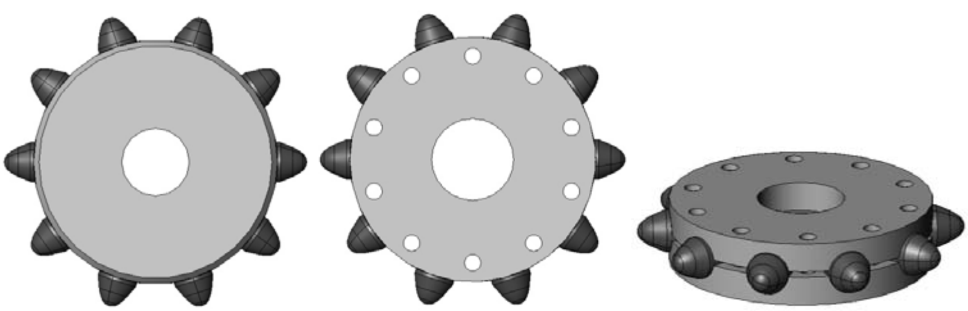

[fig56] – Dog-collar with hot fitted inserts (on the left); dog-collar with steel prop made of two halves (on the centre and right)

5.3.1.15 - Tool holder

The tool holder would keep the dog-collar in a vertical position. Two tapered roller bearings would take the vertical load while allowing the dog-collar to rotate around its axis.

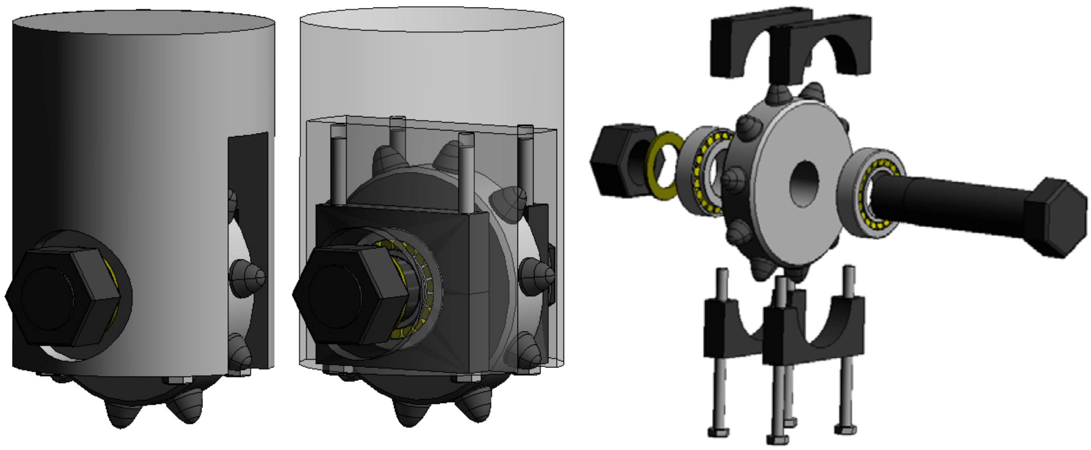

[fig57] – Dog-collar holder. Complete view; complete view with transparent prop; exploded view

This tool holder would be assembled in the tool arm [fig58]. The arm is bolted to the guide rail that would then be placed in the runner block and connected to the cylinder. The round shape of the tool holder would allow its rotation in the tool arm, thus simulating the cone shift of the drilling bits.

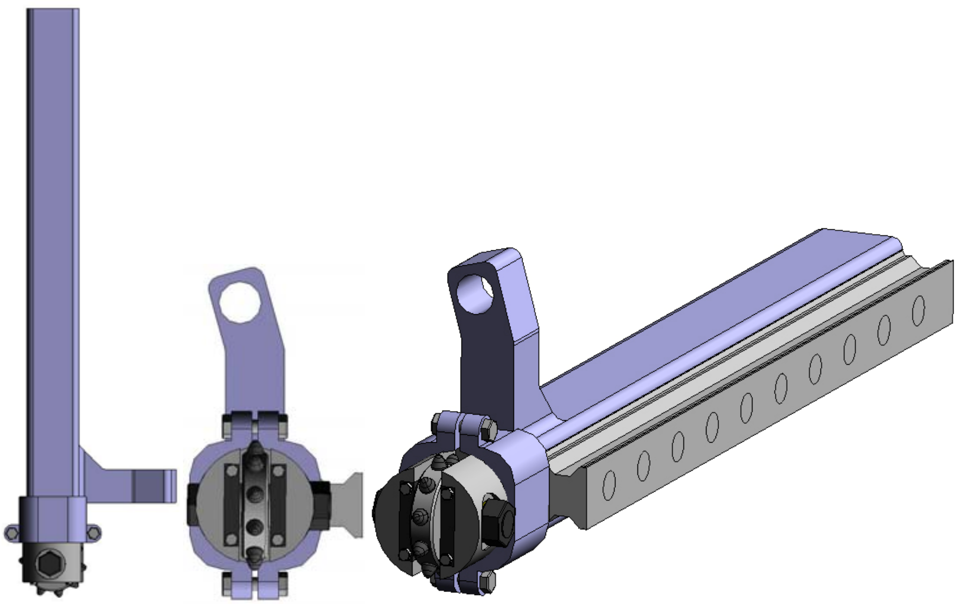

[fig58] – Tool arm with tool holder and guide rail

5.3.1.16 - Complete rig

The complete test rig would thus be composed of all the previous elements.

The floor cylinder can be easily disconnected from the turntable. The turntable is then pushed from under the frame, thus making rock loading and unloading an easier and safer operation, without risks of damaging the tool [fig62].

The overall costs can be resumed in the following table:

Turntable	8.000 €
Table cylinder	580 €
Tool cylinder	1.750 €
Frame	≈ 1.000 €
Tool holder and bearings	≈ 2.000 €
Floor guide	990 €
Tool guide	500 €
Total estimated price	**15.000€**

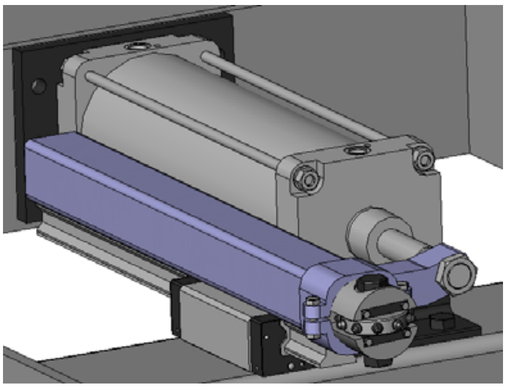

[fig59] – Tool system

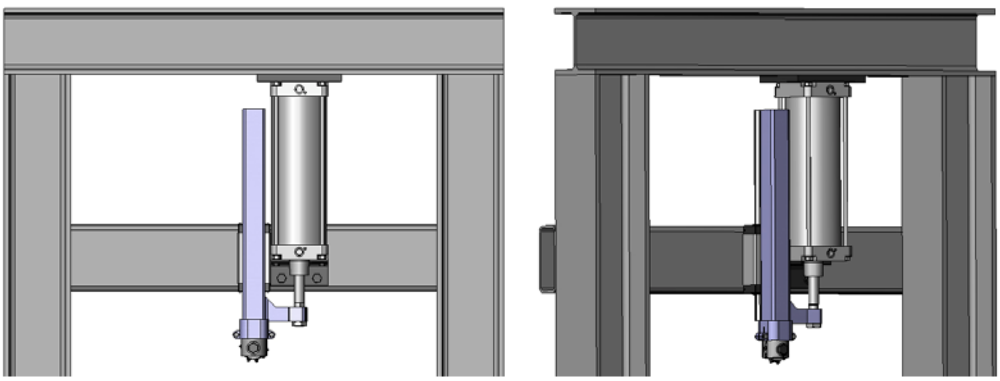

[fig60] – Tool system bolted to the frame: tool arm, tool holder, dog collar, pneumatic cylinder and guiding system

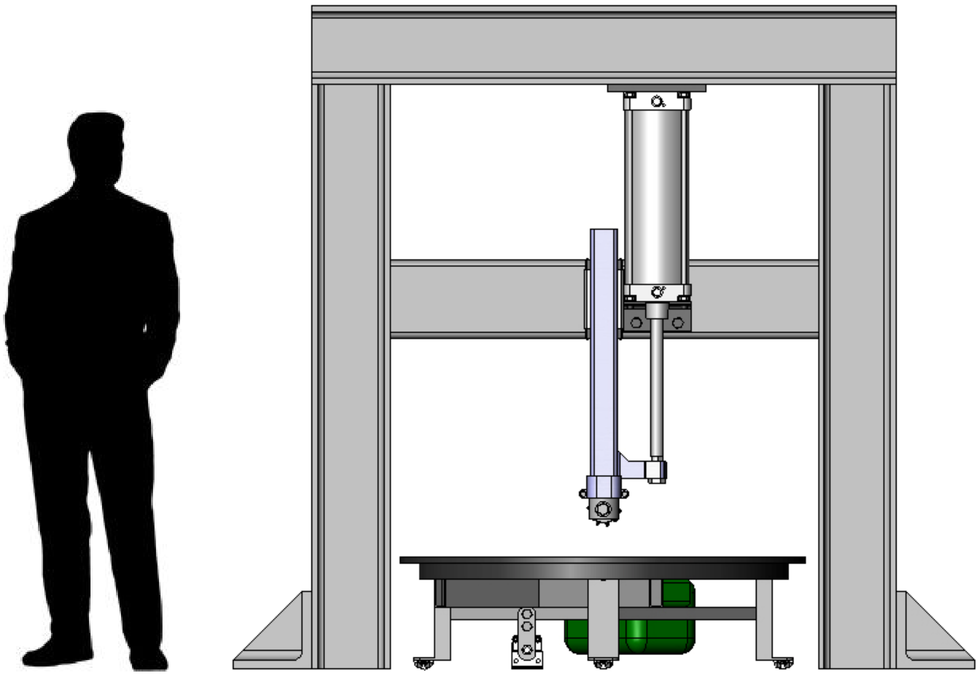

[fig61] – Complete test rig with man silhouette for dimensional comparison

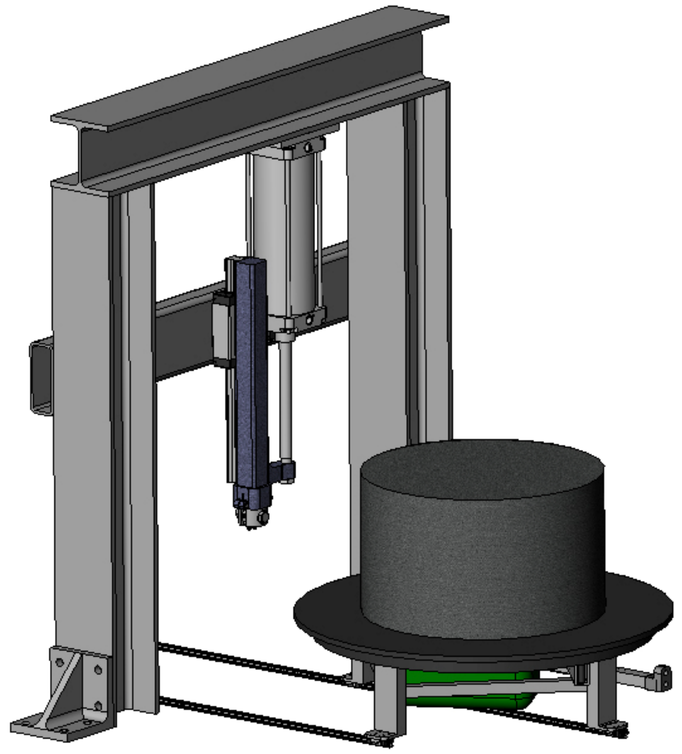

[fig62] – Test rig with table in the rock loading position

5.3.2 - Impeller-in-drum test rig design and specifications

5.3.2.1 - Abstract

The impeller-in-drum test is a both impact and abrasive wear test used to compare and evaluate different cemented carbide grades. This test has been performed by some laboratories with satisfactory results [10], [11].

It uses cemented carbide paddles that are assembled around a rotating support. This support is placed inside a rotating drum which is rubber lined. The drum is filled with a known quantity of rock and rotated slowly. Due to the rubber friction this rotation will make the stone go up and fall over the paddles. The paddles are rotated in the same direction at high speed, thus smashing the stone with the impacts.

This test is run for a certain time, after which the debris has to be taken out and replaced with new stone. After some cycles the paddles are removed, weighed and the surface is analyzed.

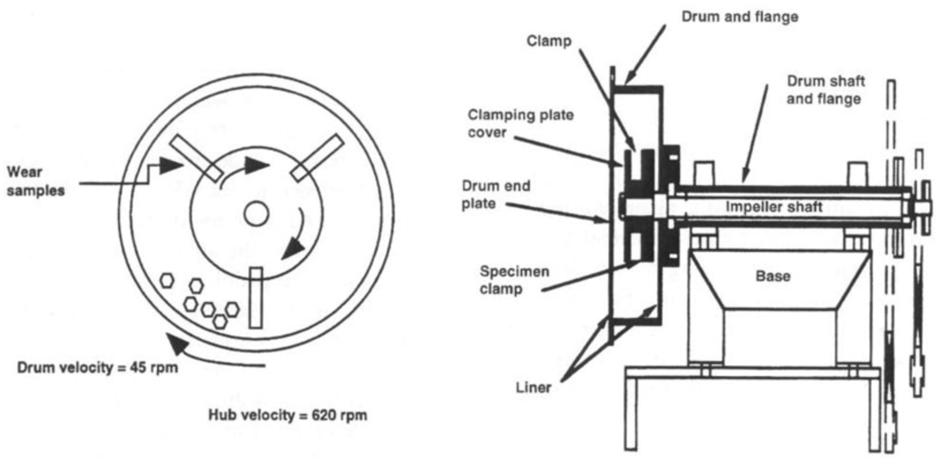

[fig63] – Impeller-in-drum test with paddle and drum rotational speeds [10]

Hexahedron cemented carbide paddles with the dimensions 75 x 25 x 12,5 mm [10], or 75 x 25 x 6 mm [11] have to be produced specifically for this test.

[fig64] – Cemented carbide test paddle

5.3.2.2 - Existing Drum

One of the reasons this impeller-in-drum test was specifically chosen to be developed at Atlas Copco Secoroc AB is that there is an available tumbling machine that can be used as drum. [See attachment #5]

This machine has a rubber lined drum, with a velocity control system. It also has a hydraulic system to pump water into the drum thru the hollow rotating axel [fig65].

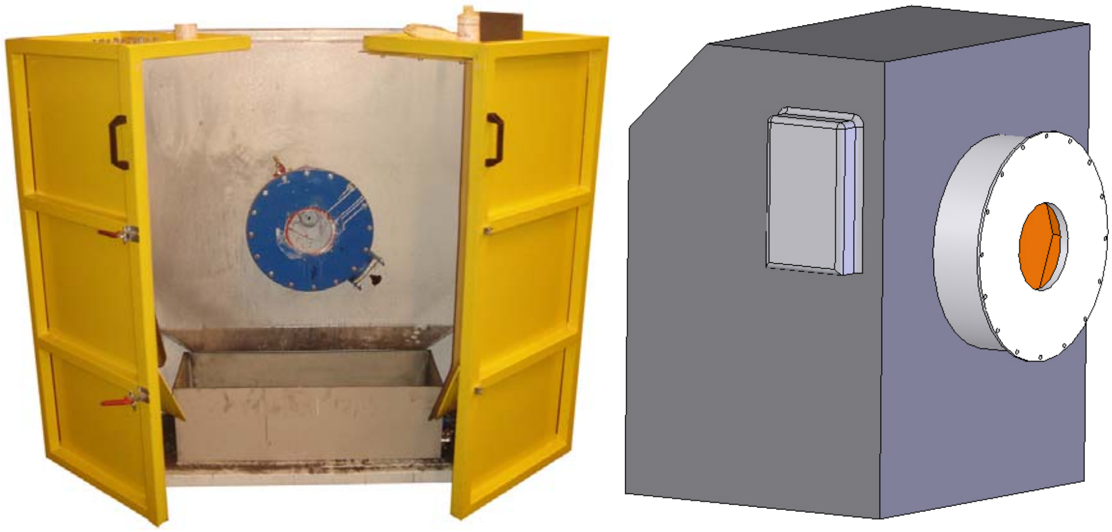

[fig65] – Existing tumbling machine that can be used as drum. 3D model side view without the yellow protection doors.

5.3.2.3 - Test specimens attainment

Test paddles with the required dimensions have to be produced for this test. They can be either supplied by some hardmetal company of produced in-house. For the objective is to evaluate different grades with accuracy, the idea of outsourcing was dropped.

The test paddles would have to be produced in the existing cemented carbide production unit. Thus, powder press tools with the required green body shape would have to be obtained. Two solutions were taken in account: produce a brand new press tool fully made of steel, or modify an old existing tool partially made of cemented carbide.

5.3.2.4 - New press tool

For the new press tool the choice was to design the green body die cavity with the dimensions: 90 x 30 x 12 mm that, after approximately 17,5% of shrinkage, would result in test paddles with the dimensions: 74.3 x 24.8 x 9.9 mm.

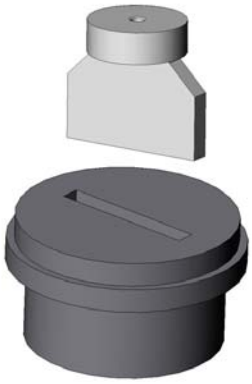

[fig66] – Powder press tool fully made of steel

In order to improve its resistance to wear, and thus its lifetime, the powder press tool die cavities and punch tips are generally made of cemented carbide. Going through frequent maintenance these press tools produce up to 150.000 green bodies a year. For the objective is not to produce a big quantity of test paddles, the press tool can be made entirely of steel.

In order to get a price estimate, the press tool technical drawings were sent to *Robustus* in Örebro. This company is currently producing most of the press tools being used in the cemented carbide production unit [see attachment #6].

The estimated price was approximately 8.000€ (the press tools with cemented carbide die cavity and punch tips cost around 15.000€).

5.3.2.5 - Old press tool

Using an old press tool would certainly reduce the costs. The cemented carbide producing unit has some tools for old products in store that won't be used. These tools made partially of cemented carbide have the required outer dimensions to fit in the powder presses. The only change to be made would be in the die cavity. The two punches would have to be made as well.

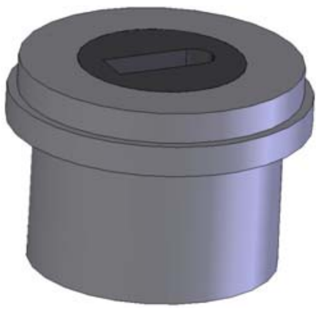

[fig67] – Existing press tool with cemented carbide die cavity

After modified, the press tool would produce green bodies with the dimensions: 70 x 45 x 19.3 mm. These, after sintering would result in paddles with: 57.8 x 37.1 x 15.9 mm.

When compared with the test paddles used in the papers [10], [11], these would be shorter, narrower and thicker. Though, this fact would not pose any problem, for the objective is not to compare results with other companies performing the same tests, but to compare results within the company.

The estimated cost for the die cavity modifications and two punches would be approximately 4.500 €.

5.3.2.6 - Paddle holder

The paddle holder would have to be a round structure with no edges on the outer surface in order to avoid impacts with the stone and thus excessive wear. It would have to be robust enough to hold the paddles in their places while hitting the stone at 620 Rpm. The decision was to draw a simple circular structure with wedged claws to hold the paddles. Four paddles will be used instead of three, making it possible to use a standard cemented carbide grade and three test grades in the same test.

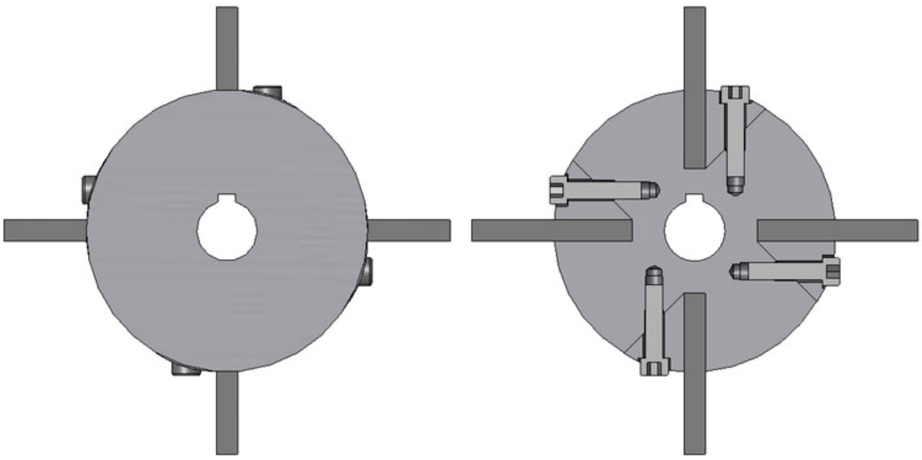

[fig68] – Paddle holder with four paddles

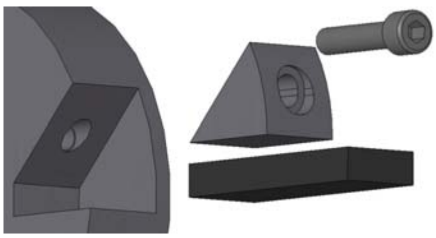

[fig69] - The wedged claws would be fastened to the rotating holder

5.3.2.7 - Whole assembly

For the rotational movement of the paddle holder an electric motor would have to be used. In the existing solutions the paddle holder axel goes through the hollow drum axel. Given the small diameter of the existing drum axel bore, this solution could not be applied in this case. The motor would have to be assembled through the front drum cavity.

The easiest way would be to build a support table to hold the motor, where it could slide back in order to replace the stone or the paddles. This table would have four clamps to hold the motor while performing the test.

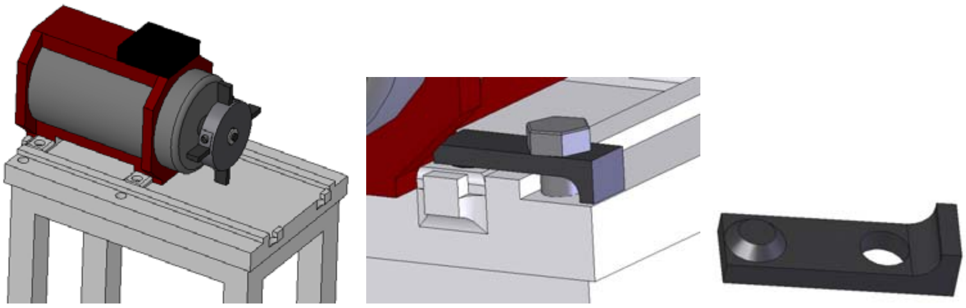

[fig70] – Electric motor with paddle holder and support table. Clamping system. Steel clamp.

A debris shield would have to be made in order to prevent the debris from going out of the drum.

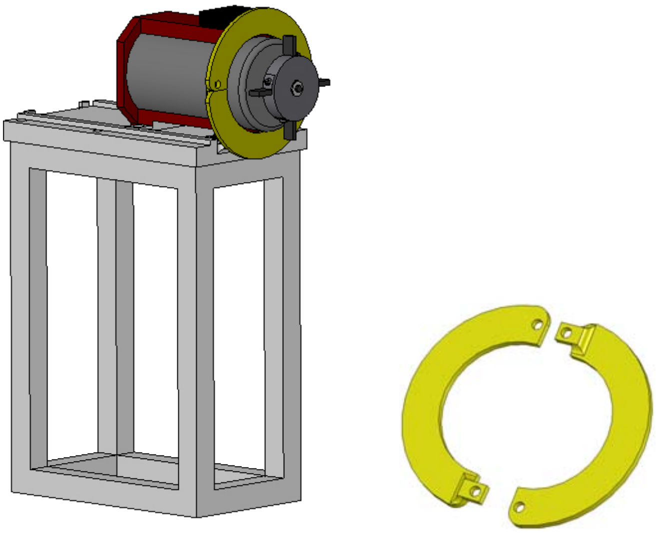

[fig71] – Electric motor with paddle holder and debris shield. Polymeric debris shield made of two halves

The choice was to use a simple three-phase electric motor connected to a variable-frequency drive. This would control the electric power frequency, and thus the rotational speed. The vibration resulting from the paddles impact could damage the electric motor. Thus, a motor with heavy duty bearings on the drive-side would have to be chosen.

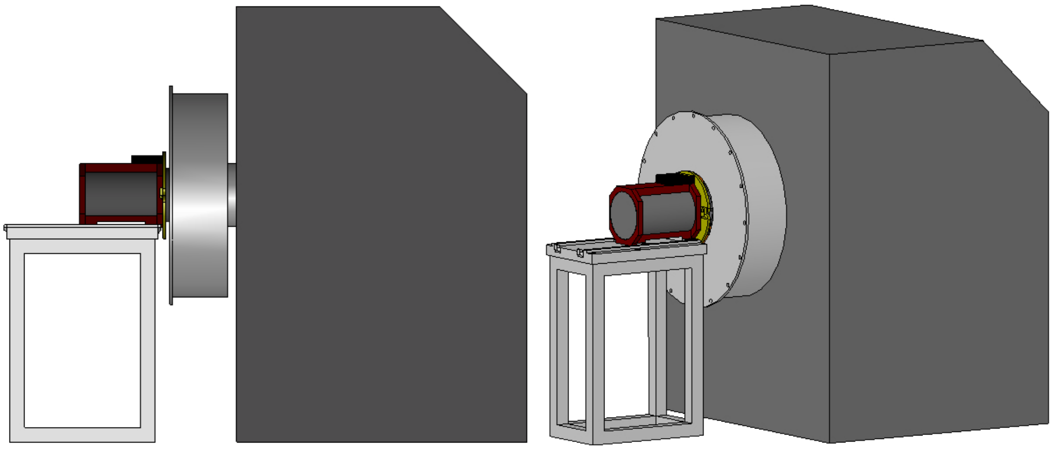

[fig72] – Impeller-in-drum complete test rig

The overall costs for the complete rig, considering the choice of an old press tool, can be resumed in the following table:

Support table	300 €
Paddle holder and debris shield	550 €
Press tool	≈ 4.500 €
Motor and electric drive	≈ 1.000 €
Total estimated price	**6.500€**

5.4 - Field testing

Field testing is the ultimate testing the cemented carbide inserts can undergo. In Atlas Copco Secoroc AB these tests are always performed by the costumers, with or without supervision from the company. For a considerable number of variables has to be noted down while performing these drilling tests, the costumers need to be trustworthy. They have to record the rate of penetration, the weight on bit, the rotational speed, the drilled distance, etc. Though it might be a laborious task to drill and take note of all these parameters at the same time, most of the companies are willing to perform these tests. They generally get free equipment that can do the job as well as the commercially available they would have to buy.

When testing a whole new product, when the number of variables to be recorded is too high, or when special care has to be taken while drilling, these tests are fully supervised by an Atlas Copco engineer.

[fig73] – Surface and underground drilling tests

6 - Wear analysis

The wear analysis plays an important role in the cemented carbide testing. All the previously discussed test methods would render unfruitful without subsequent analysis. It has to be done following accurate guidelines in order to obtain comparable results, thus enabling the evaluation of different tested grades.

The main and most basic method for wear evaluation in the test samples is the **weighing**. Virtually all the wear tests use the weight of the samples as the prime parameter. It depicts the amount of lost material, thus proving a good initial idea of the wear extent. The simplicity and reliability of this method are the main advantages of the weighing analysis. The fact that some inserts are hot fitted in the steel shank might hinder the specimens from being removed though. This reason renders weighing unrealizable in some certain tests.

For those tests where the removal of the inserts is cumbersome the **3D laser scanning technique** can be used. It is a surface analysis method that can be used to determine the amount of worn-out material. Given its high-accuracy and non-destructivity characteristics, it is an advantageous method when applied to the wear evaluation of cemented carbides.

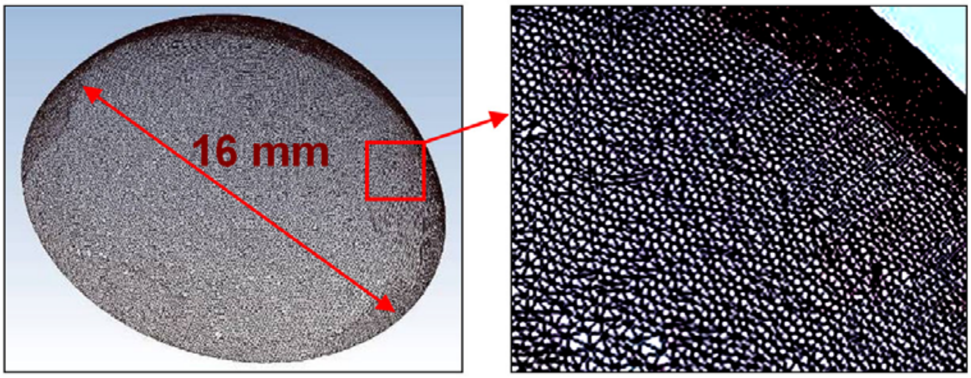

[fig74] – Drilling insert tip image obtained through laser scanning

Another widely spread method is the electron microscopy, namely the **scanning electron microscope (SEM)**. Although no quantitative results are obtained, the qualitative surface analysis is a good method to evaluate the wear rate. The different deterioration and detachment mechanisms can be identified as well as the influence of the different rock types.

Homing cross sectioning [12] is a preparation technique used to reveal the weakest zones of the cemented carbide inserts. Instead of the traditional cross-section preparation where the insert is cut in a specific location, here a small groove is made and the insert is subsequently breached in two halves with a wedge. The crack will naturally follow the easiest path, thus revealing the weakest zones. This technique is specifically suitable for the study of the rock penetration mechanisms in the surface layers. Given the unevenness of the resulting crack surface this method is primarily intended for studies in the SEM [13].

[fig75] – Homing cross-sectioning crack surface showing rock material deeply intruded into the cemented carbide structure (obtained with SEM)

7 - Conclusions

In conformity with the initial objectives, practical solutions were found for both the dog-collar and impeller-in-drum half-field wear tests.

Although it was not built, the dog-collar test rig could be easily attained using this work as guideline. The necessary components were chosen and designed as function of the initial requirements. All these requirements were met, keeping the overall costs considerably under initial budget.

When compared with the existing solutions, this homemade test rig would not only be cheaper but also simulate the real conditions more accurately. A considerable amount of work load would be necessary and some problems would probably arise with the progress of the machine assembly. Though, no major issues are expected.

The impeller-in-drum test rig was also fully projected. The decision of using an old press tool or building a new one remained to be made. Other than that, all the necessary components were designed using the references [10] and [11] as guideline. The electric motor and frequency drive were not chosen for this choice would be made by the company's supplier of electric components.

During the course of this project I had the chance to get acquainted with most of the rock drilling aspects. I observed the production of both rotary crushing and percussive drilling equipment, as well as the production of the cemented carbide inserts. I've acquired extensive knowledge about most of the different production parameters to be controlled. I've also had the chance to witness closely both surface and underground drilling. I've learned about the different drilling equipment, drilling techniques and procedures. The daily contact with the R&D teams enabled the understanding of the different phases of product development. All in all this apprenticeship, for which I am truly gratified, played a vital role in the development of this project.

References

[1] U. Beste (2004): *On the nature of cemented carbide wear in rock drilling.* Acta Universitatis Upsaliensis, Uppsala, Sweden.

[2] L. Nyman (2007): *Master of Science program in materials engineering - Thesis - Development of a test for measuring wear of cemented carbide in rock drilling applications.* Uppsala Universitet, Uppsala, Sweden.

[3] H. E. Exner (1979): *Physical and chemical nature of cemented carbides*. Max-Planck-Institut für Metallforschung, Institut für Werkstoffwissenschaften, Stuttgart, Germany.

[4] U. Beste, S. Jacobson (2002): *Friction between a cemented carbide rock drill button and different rock types*. Uppsala Universitet, Uppsala.

[5] B. Uhrenius (2000): *Pulvermetallurgi*. Institutionen för Materialvetenskap, Kungl Tekniska Högskolan, Stockholm.

[6] W. D. Schubert, H. Neumeister, G. Kinger, B. Lux (1997): *Hardness to toughness relationship of fine-grained WC-Co hardmetals*. Institute for Chemical Technology of Inorganic Materials, Vienna University of Technology, 1060 Vienna, Austria

[7] Ching-Ray Chang, J. P. Shyu (1990): *Effects of Porosity on Coercive Force of Particulate Medium*. Department of Physics, National Taiwan University, Taipei, Taiwan

[8] N. Sacks, I. Northrop, C. Allen (1997): *Fracture toughness on 'nanocrystalline' WC-Co hard metals*. Department of Materials Engineering. University of Cape Town, South Africa.

[9] H. Engqvist, U. Wiklund (2000): *Mapping of mechanical properties of WC–Co using nanoindentation*. Uppsala Universitet, Uppsala, Sweden.

[10] R. D. Wilson, J. A. Hawk (1999): *Impeller wear impact-abrasive wear test*. US Department of Energy, Albany Research Center, USA.

[11] S .Kiani, J. W. Bitler: *Comparative study on wear behaviour of sintered WC-Co.* Kennametal Inc, USA.

[12] U. Beste, S. Jacobson: *Homing cross sectioning – a technique to reveal weak zones in worn surfaces*.

[13] U. Beste, S. Jacobson: Targeting micro-sectioning – A technique to study subsurface features in worn specimens. Atlas Copco Secoroc AB, Fagersta, Sweden; Tribomaterials Group, Uppsala University, Sweden.

List of figures

Attachments

#1 – Tool pneumatic components

#2 – Table pneumatic components

#3 – Paper: S .Kiani, J. W. Bitler: *Comparative study on wear behaviour of sintered WC-Co.* Kennametal Inc, USA.

#4 – Paper: R. D. Wilson, J. A. Hawk (1999): *Impeller wear impact-abrasive wear test*. US Department of Energy, Albany Research Center, USA.

#5 – Tumbling machine technical drawing

#6 – Press tool technical drawing

Attachment #1

Tool pneumatic system – Components

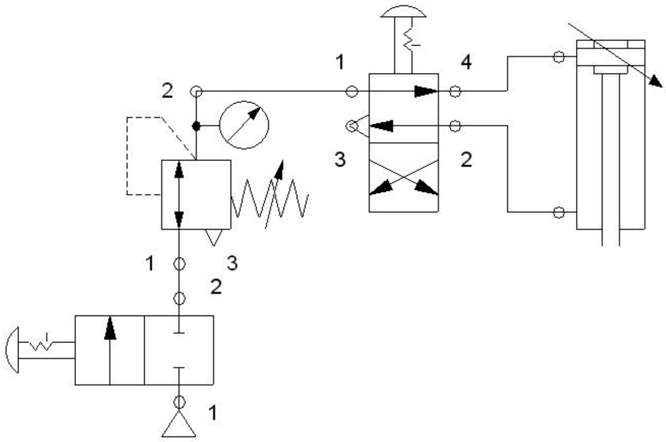

Complete pneumatic diagram

Pneumatic cylinder

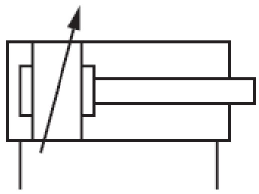

- Tie rod cylinder, ISO 15552, Series ITS - 5238001000
- Double-acting; cushioning: pneumatic, adjustable; piston rod: external thread
- Piston: Ø200
- M36x2 piston rod thread
- Stroke: 500mm
- Ports G3/4
- Price: 1068,14 €

Flange mount

- Flange mounting MF1, MF2 - 1827001461
- Price: 134,35€

Foot mount

- Foot mounting MS1 - 1827001458

- Price: 116.62€

4/2 way valve manually operated

- 5/2-way valve, Series 563 131 - 5631310100
- Ports: G1/4
- 128,16€

2/2 way valve manually operated

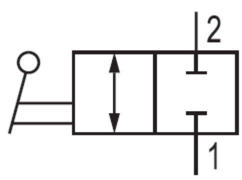

- 2/2-way stop valve, Series SC01 - 1823391907
- Ports: R1/4 - G1/4
- Price: 22.02€ (2 units)

Pressure control valve with manometer

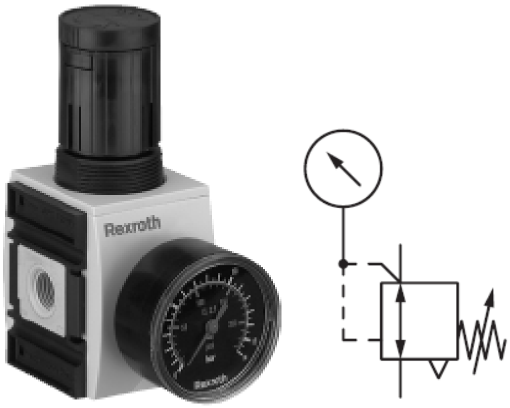

- Pressure regulator, Series AS2-RGS - R412006143
- Ports: G1/4
- Price: 67€

Exhaust silencer

- Silencers, Series SI1 Sintered bronze - 1827000033
- Port: G1/4
- Price: 42,25€ (10 units)

Port adaptor

- Double nipple - 1823391286
- Ports: G3/4 to G1/2
- Price: 19.75€ (2 units)

<u>G1/2 port to push fit Ø10 port adaptor</u>

- Series QR1-S Standard – 2121010120
- Ports: G1/2 to Ø10
- Price: 56,53€ (10 units)

<u>G1/4 port to push fit Ø10 port adaptor</u>

- Series QR1-S Standard - 2121010140
- Ports: G1/4 to Ø10
- Price: 35,70€ (10 units)

<u>Air hose</u>

- Compressed air hose, Series TU1-S - 1820712005
- Diameter: Ø10
- Price: 63,96€ (25 meters)

Total price: 1754,48 €

Attachment #2

Turntable pneumatic system - Components

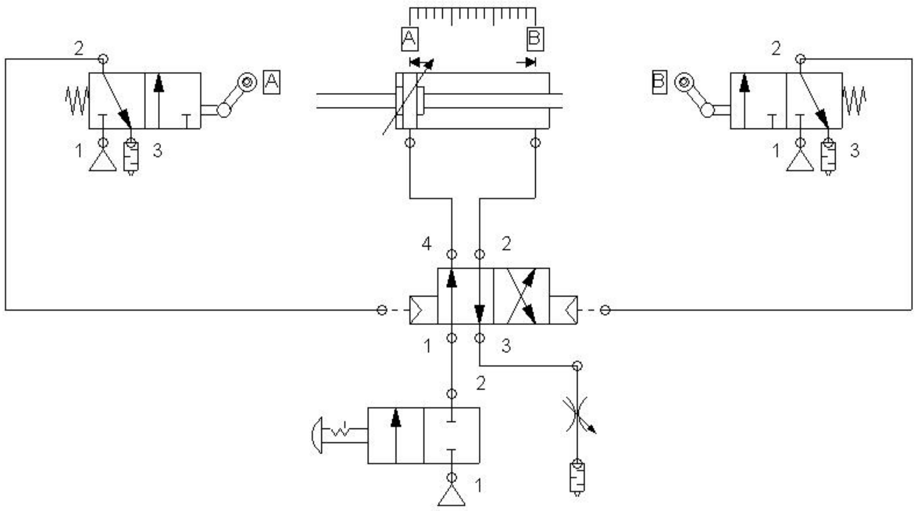

Complete pneumatic diagram

The use of a symmetric double acting pneumatic cylinder is necessary in order to induce the same speed in both directions

Pneumatic network available. Average pressure of 6 bars that can drop to 5.5bar.

The following components were chosen from Bosch Rexroth, as it supplies all the necessary pneumatic equipment. An advantage is that all the detailed characteristics, drawings and prices can be obtained online.

<u>Pneumatic cylinder</u>

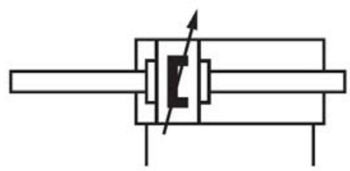

- Profile cylinder, ISO 15552, Series PRA - R480041497
- Double-acting; with magnetic piston; cushioning: pneumatic, adjustable; piston rod: through, external thread
- 80 mm piston diameter
- 25 mm piston rod
- M20x1,5 piston rod thread
- Ports: G3/8
- Stroke: 600m
- Price: 284.70€

Foot mounting (2 units)

- Foot mounting MS1 - 1827001275
- Price: 24.87€ (2 units)

3/2 way valve mechanically actuated and spring returned (2 units)

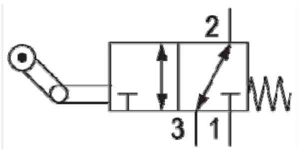

- 3/2-way valve, Series ST - 0820402003
- Port: G1/8
- Price: 63.37€

Silent exhausts (3 units)

- Silencers, Series SI1 - 1827000000
- Port: G1/8
- 21.42€ (5 units)

4/2 way valve pneumatically actuated

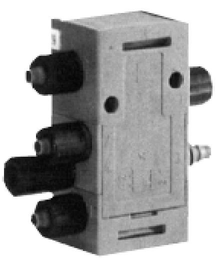

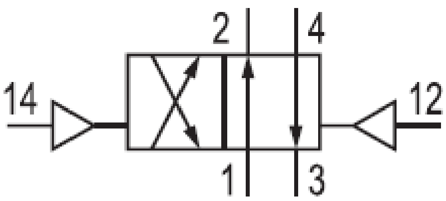

- 4/2-way valve, Series 840 - 5718410000
- Push-in fitting
- Price: 53.43€

<u>2/2 way valve manually actuated</u>

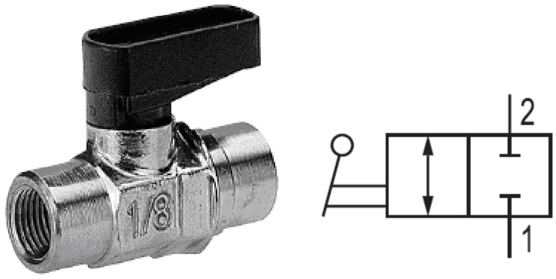

- 2/2-way stop valve, Series SC01 - 1823391910
- Ports: G1/8
- 21.42€ (2 units)

<u>Throttle valve</u>

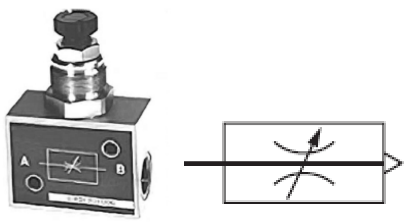

- Series CH01 – 0821201004
- Ports: G1/8
- 22.13€

<u>Flow divider</u>

- Cross connection - 1823390041
- Ports: G1/8
- 13.45€ (2 units)

Push in fittings

- Series QR1-S Mini - R412005125
- Ports: G1/8 to D6
- Price: 53.55€ (25 units)

Air hose

- Compressed air hose, Series TU1 – 1820712201
- Diameter: 6mm
- 19.34€ (25 meters)

Push in fitting for cylinder 3/8

- Series QR1-S Standard - R412005000
- Ports: G3/8 to D6
- 33.92€ (10 units)

Total price: 575.6€

Attachment #3

Paper: S .Kiani, J. W. Bitler: *Comparative study on wear behaviour of sintered WC-Co.* Kennametal Inc, USA.

Comparative study on wear behavior of sintered WC-Co

Sara Kiani and Jonathan W Bitler

Kennametal Inc.

ABSTRACT

To more accurately understand the behavior of cemented carbides in applications where both impact and abrasion can cause premature failure, an alternative to standard ASTM wear tests is evaluated. The novel test, developed by NETL-Albany, is called impact abrasion and uses a rotating drum to create impact. It differs from B611 and G65 methods, since it offers a combination of impact and wear and, thus, an ability to identify potential issues with chipping events in carbides. Certain applications require both high toughness and high wear resistance materials for superior performance, for example, cobalt cemented carbides used in oil and gas drilling where the strata can vary significantly. Wear resistance of ten carbide grades was measured using the three procedures. Impact abrasion method can more distinctively predict accelerated wear of tough grades as well as chipping behavior of brittle carbides. In summary, the impact abrasion procedure may, in certain applications, be a more useful laboratory test for predicting field behavior than standard ASTM tests.

INTRODUCTION

WC-Co hardmetals are widely used for wear resistance applications like mining, drilling, earth moving, mineral processing, and metal cutting. Tungsten carbide grain size, as well as the content and composition of the metal binder (generally Co), strongly influence physical and mechanical properties including wear resistance. Wear resistance of a material depends on the material's resistance to penetration by abrasive particles or protruding asperities of mating material, and the difficulty of material removal by fracture and plastic flow.[1]

In cases when the abrasive is softer than the hardmetal, the wear mechanism is removal of the binder phase, followed by fragmentation of the carbide grains with gradual removal of these fragments until the whole grain is removed. It is suggested that wear rate is directly related to binder mean free path in soft abrasion.[2]

In general, minimizing the mean free path in the binder phase by decreasing the carbide grain size and/or the binder content leads to an increase in resistance to plastic deformation in the binder phase. There is a good correlation between wear resistance and mean free path as well as compressive strength of WC-binder composite and normal force applied to the wear surface.[3]

In abrasion of conventional cemented carbides, surface shearing and grooving displaces the carbide grains, leading to an extrusion of the cobalt binder phase towards the surface. The carbide grains thus lose their binder phase support and slip, fracture or fall out of the surface. There will be plastic deformation and micro-cutting to a much higher extent than ceramics.[4]

In other words, abrasive wear can be produced by plastic deformation or brittle fracture. Plastic deformation can be seen as cutting and ploughing modes. The main difference between them is that cutting mode needs high attack angle, while ploughing needs low. When the abrasive particles are in contact with the surface, scratches are formed producing grooves and leading to plastic deformation. Brittle fracture on the other hand, involves the presence of cracks in the surface and subsurface. Brittle fracture is referred to pullout of the carbide grains, Palmqvist cracking and spalling.[5]

When specifically characterizing wear in rock drilling, four mechanisms are involved:
Surface impact spalling
Surface impact fatigue spalling
Thermal fatigue
Abrasion

The two former spalling mechanisms are most dominating when drilling hard and abrasive rock types such as quartzite and granite. The thermal fatigue is dominant when drilling in soft non-abrasive formations such as calcite and magnetite, and abrasion mechanism dominates the wear when drilling in soft but abrasive rocks, such as sandstone.[6]

Abrasion wear process has been divided in to two main categories; high stress grinding abrasion (i.e., the abrasive particle is crushed during the wear interaction), and low stress scratching abrasion (i.e., the abrasive particle remains intact as it moves freely across the wear surface). ASTM B611 and ASTM G65 cover these two wear regimes respectively.[7]

Abrasion can be accelerated when impact is involved. These two factors contribute to faster material degradation and loss. Hence for the purpose of this study a laboratory impact-abrasion test has been developed using information published by NETL-Albany Research Center.[8]

The original concept developed by Bond was to use an apparatus to predict wear, and hence the energy consumption that occurred during the crushing and grinding of ore. The Albany Research Center modified Bond's impact pulverizer design to better simulate a wear-testing device instead of a machine used solely for determining the abrasive index of rocks. The major change was to add a three-paddle impeller hub assembly instead of one. Overall, this test method bridges the gap between the purely abrasive wear tests and the high stress gouging wear tests.[8]

In general, ASTM wear test methods are not fully capable of predicting actual wear behavior of cemented carbide grades in the field. For example, alumina sand used for ASTM B611 test is not always as abrasive as formations found in mining applications, and silica used in ASTM G65 is definitely less abrasive than most of the drilling formations. Knowing this, gave authors motivation to study wear behavior of various cemented carbide grades under both impact and abrasion of rocks like quartzite. This test is a more realistic simulation to the field, as actual field test is rather time consuming and non-economical. Data obtained may help in grade selection especially among high toughness grades used in oil and gas drilling, coal mining, road construction, etc.

EXPERIMENT

Impact-abrasion wear apparatus

The test apparatus is a rotating impeller in drum shown in figure 1. Based on the current design, three specimens can be tested simultaneously. The specimens are 76 x 25 x 6 mm (3 x 1 x 0.24 inch) rectangular bars.

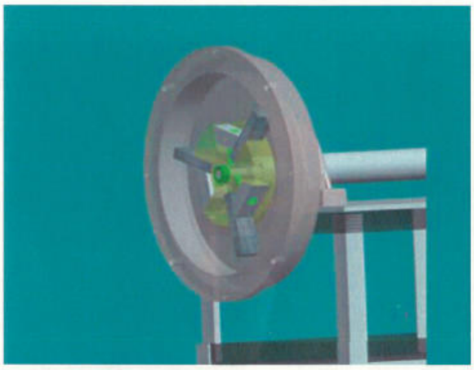

Figure 1. Three specimens are mounted on the impeller that rotates inside the hub. Hub is designed to hold 0.6 kg (1.3 lbs) of ore.

Both impeller and drum rotate clockwise at 620rpm and 45rpm respectively. Large drum is rubber-lined to reduce noise and provide some friction between the ore and the drum. Ore is lifted when the drum rotates to the point where it overcomes the frictional forces of the lining and falls in to the path of rotating paddles. Test can accommodate any type of rock like quartzite, calcite, limestone, etc. Size of the rock is in the range of 19-32mm (0.75-1.25 inch) based on the previous work.[8] Pink quartzite rock (98% SiO_2) supplied from L. G. Everist, Inc. has been used for the purpose of this research.
Results include average cumulative volume loss and volume loss per hour as a function of hardness. Test is done three times for each grade of carbide to better demonstrate the repeatability.

Material and sample preparation

For this study ten grades of cemented tungsten carbide ranging from 6% to 16% cobalt have been prepared. For testing, 76 x 25 x 6 mm (3 x 1 x 0.24 inch) bars are pressed, sintered and ground on two faces. Grades used for this project are listed in table 1. Microstructure of grades with the highest and lowest hardness, based on table 1, is shown in figure 2.

Table1. Grades selected for testing.

Grade	%Co	Hardness (HRA)
1	6	90.8
2	9	89.9
3	11	89.4
4	11	88.4
5	10	88.1
6	12	87.1
7	12	85.5
8	16	85.3
9	20	84.2
10	16	83.7

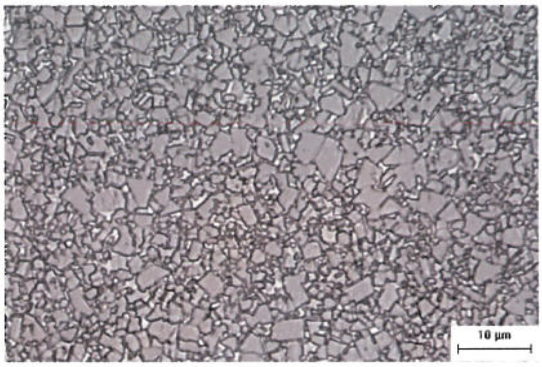

(a)

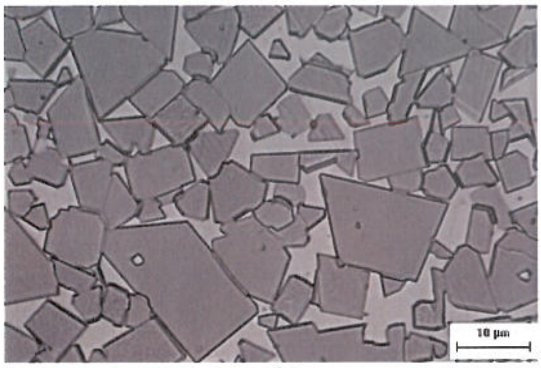

(b)

Figure 2a. Microstructure of the grade with 90.8 HRA, b. Microstructure of the grade with 83.7 HRA.

Test procedure

Multi-hour test method has been used for the purpose of this study. In this method, only one side of the sample is tested or impacted by the ore. Test is run for a total of 4 hours. Every hour parts are removed, cleaned and weighed. Every 15 minutes the used ore is replaced with fresh ore. Figure 3 illustrates the deformation on quartzite ore after the first 15 minutes of testing. In general ores tend to break down and lose their sharp edges.

(a)

(b)

Figure 3a. Quartzite ore before the test with sharp edges, b. Quartzite ore after 15 minutes with round corners

RESULTS

It is known that tough cemented carbide grades are resistant to impact but do not have good abrasion resistance. The opposite is valid for harder grades. Correlation of hardness to impact and abrasion resistance is schematically shown in figure 7.

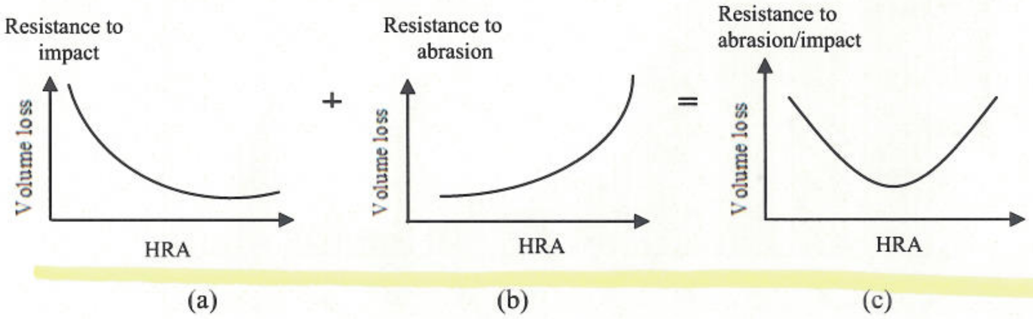

Figure 7a-b. Resistance to impact is inversely and resistance to abrasion is directly proportional to hardness, c. When both abrasion and impact phenomena are involved.

Average cumulative volume loss as a function of hardness is presented in figure 8.

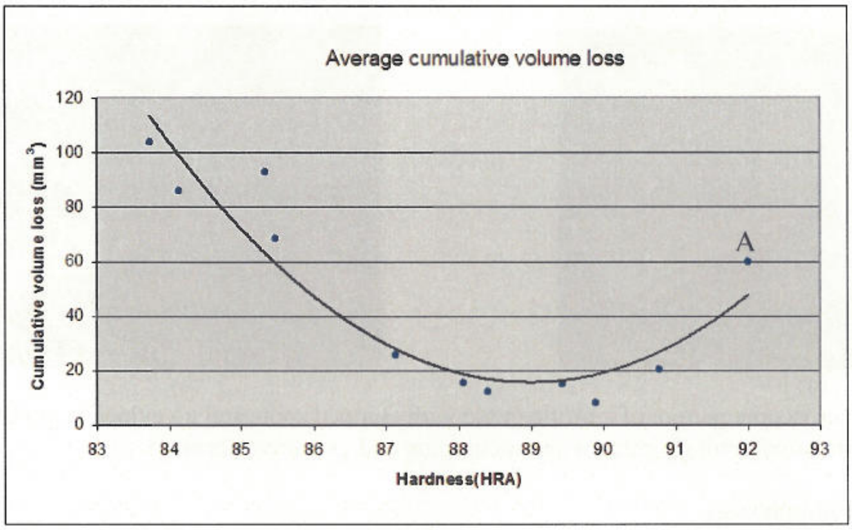

Figure 8. Average cumulative volume loss versus hardness.

Data shows a distinctive volume loss along the hardness range. Tough grades show high volume loss due to low resistance to abrasion. Volume loss decreases towards brittle grades. For grades with 90 HRA and above, amount of volume loss increases again as a result of poor impact resistance (chipping). Point A corresponds to a very brittle grade that fractured during the 3rd hour of testing. This grade is not included in table 1, however the data show the dominant chipping phenomena for this grade. This graph correlates well with the schematic trend shown in figure 7 for impact abrasion wear test. To demonstrate volume loss with respect to time for each grade, bar chart graph has been used (figure 9).

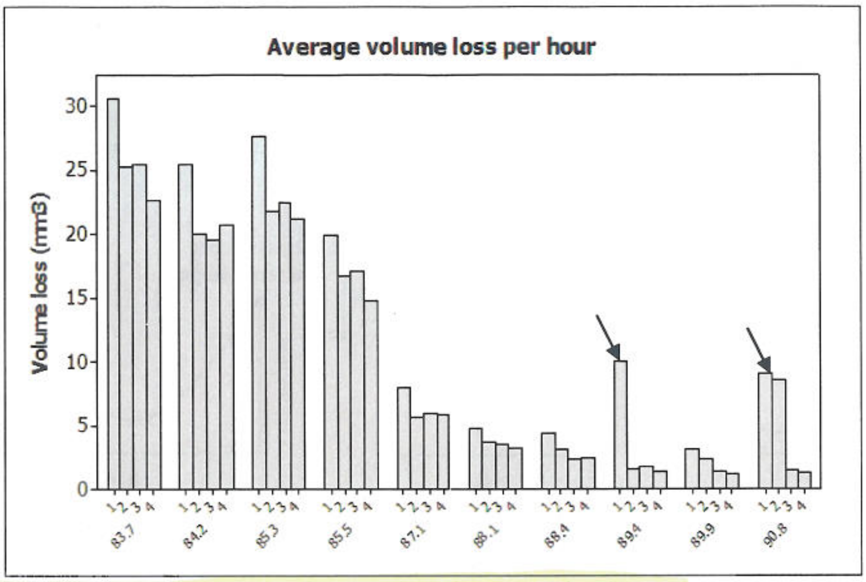

Figure 9. Average volume loss per hour for tested grades versus hardness.

Brittle grades have chipping in the first or second hour of testing that results in high volume loss (indicated with arrows in the graph). Figure 10 compares a brittle and a tough grade after a 4-hour of wear test.

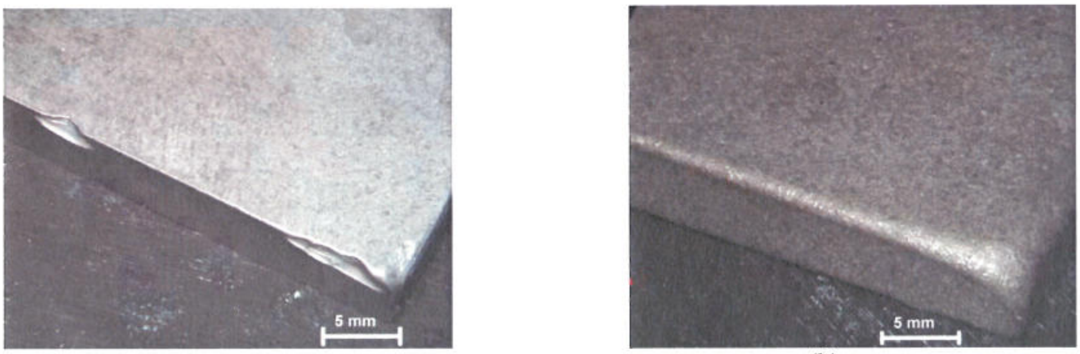

(a) (b)

Figure 10a. Macroscopic picture of a brittle grade with chipped spots and no evidence of abrasion, b. Macroscopic picture of a tough grade without chipping and excessive abrasion.

SEM and wear morphology

As mentioned in the introduction, abrasive wear can be produced by either plastic deformation or brittle fracture. Pictures taken with scanning electron microscope focuses on grains' plastic deformation, grain pull out and binder extrusion to the surface. Figures 4-5 illustrate morphology of the wear surface for a typical brittle and tough grade after testing. The brittle grade contains 6% cobalt and the tough grade contains 16% cobalt.

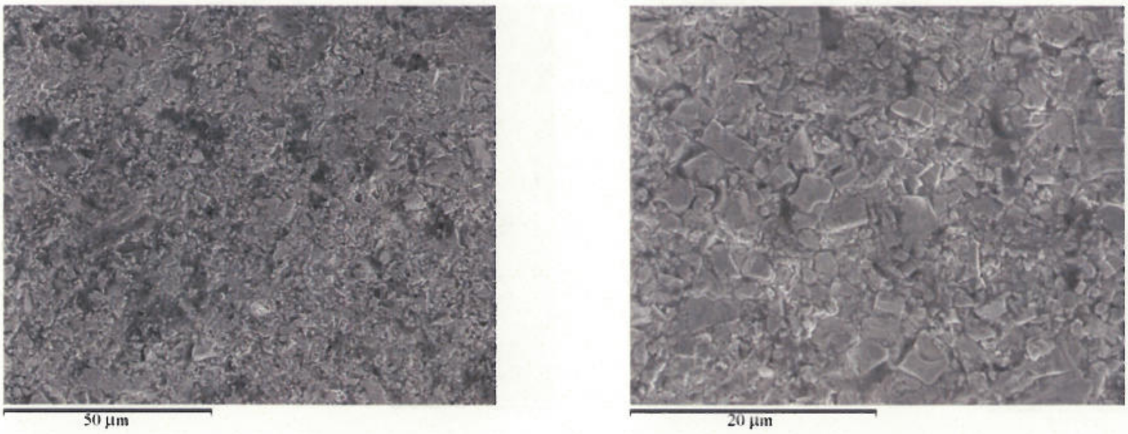

(a) (b)

Figure 4. Wear morphology of a brittle grade after a 4-hour of impact abrasion wear test at a. 1000x, b. 3000x.

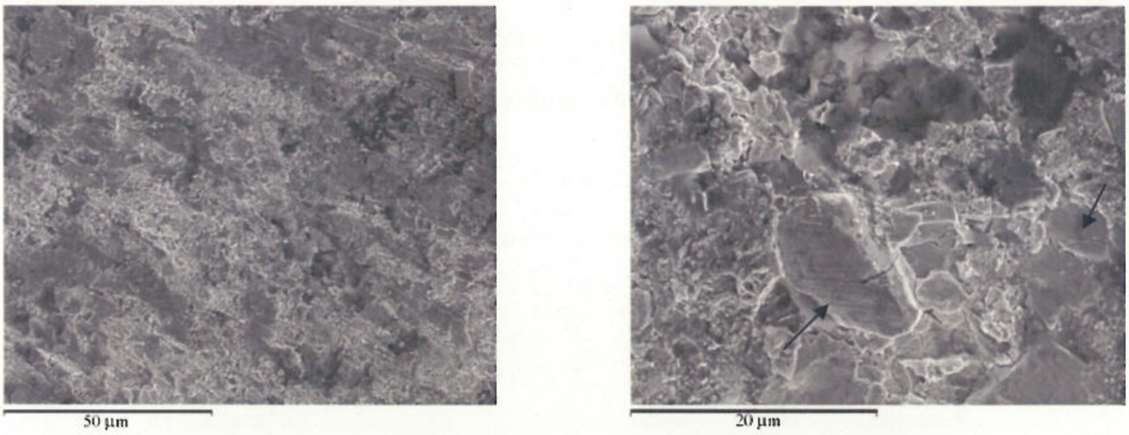

(a) (b)

Figure 5. Wear morphology of a tough grade after 4-hour of impact abrasion wear test at a. 1000x, b. 3000x.

Brittle grades have little evidence of surface damage to WC grains and no sign of binder pull out or grain deformation. High abrasion resistance help in maintaining an intact surface, while corners and edges chip due to poor resistance to impact. On the contrary, tough grades are severely damaged. Binder pull out causes grain dislodging. Micro cracking (indicated with arrows on figure 5b) will eventually lead to crushed grains. Also dislocation steps resulting in plastic deformation is obvious on all the large grains. In addition, a button taken from rock drilling (coal overburden) bit was analyzed. These drill bits use cylindrical buttons of cemented carbide inserted into a steel body to enhance the wear resistance. Similar wear morphology is seen on parts subject to impact abrasion wear test and buttons pulled out from bit after drilling. Figure 6 compares wear morphologies at 4000X.

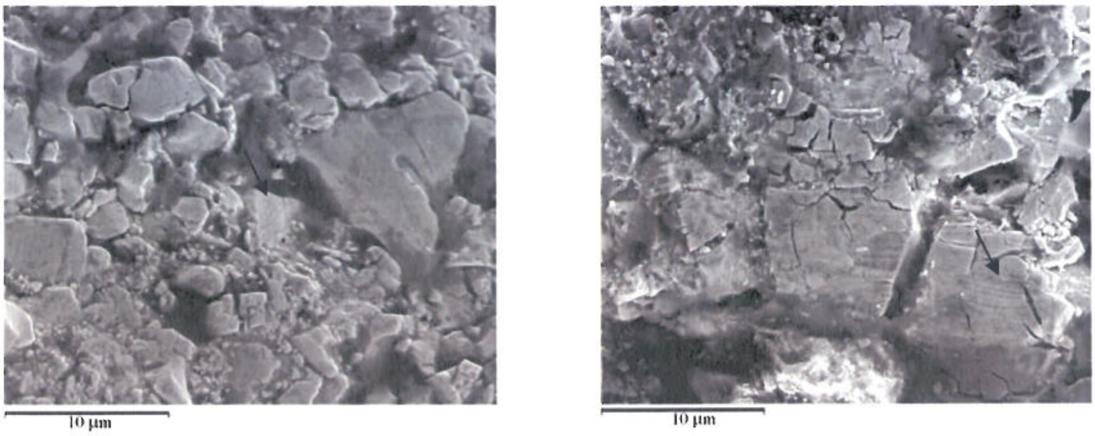

(a) (b)

Figure 6. Wear morphology of a. button from rock drilling bit, b. A tough grade with 83.7 HRA (table 1).

Crushed grains, plastic deformation especially on the large grains due to dislocation steps (indicated with arrows in the figure) and binder pull out are dominant wear mechanisms in both parts.

In addition to compare these results to ASTM B611 and G65 procedures, same bars are cut in half, and the untested surface is used.
Grades listed in table 1 are tested three times, and average volume loss versus hardness for each test is plotted in figures 11 and 12.

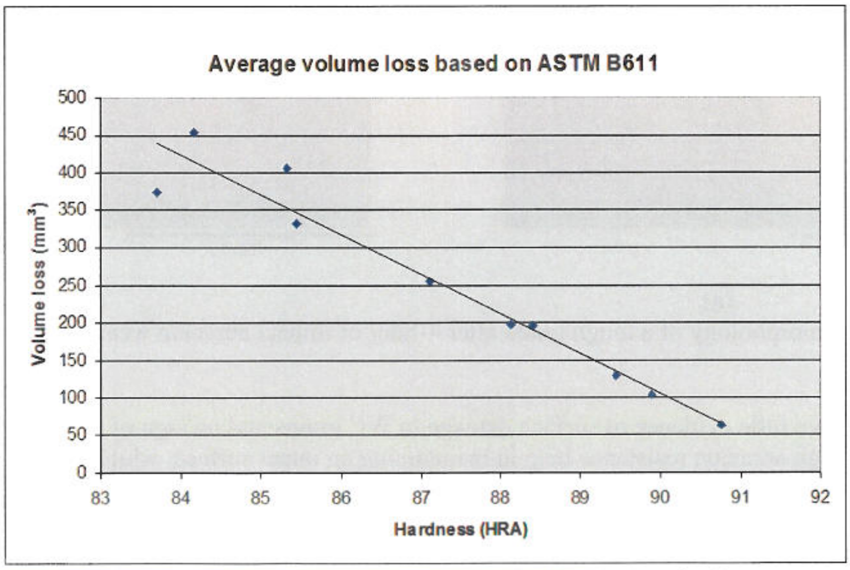

Figure 11. Average volume loss versus hardness based on ASTM B611 method.

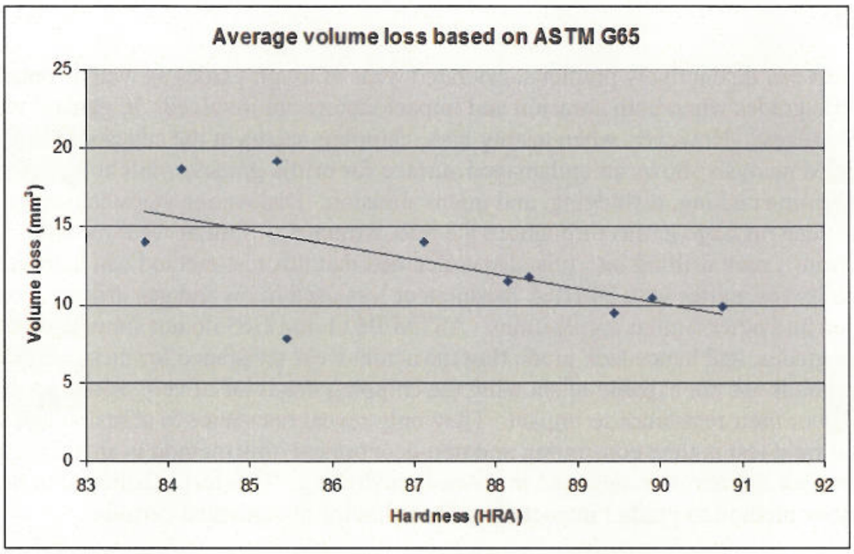

Figure 12. Average volume loss versus hardness based on ASTM G65 method.

ASTM B611 shows a linear correlation between wear resistance and hardness. It is the most abrasive test among the three procedures, and has been historically used to characterize wear behavior of cemented carbides. However, it only reveals resistance to abrasion, and hence lack the effect of impact forces engaged in drilling, mining, construction, etc.
ASTM G65 is the least abrasive test. Difference in volume loss along the hardness range (from tough to brittle grades) is not significant compared to impact abrasion wear test (figure 8) and ASTM B611 (figure 11). This test is an indicator of resistance to scratching, and hence not a very common test for cemented carbides.

Typical wear scar of a brittle grade after ASTM B611 and G65 test is shown in figure 13. Tough grades have similar but deeper wear scars. These pictures are included for comparison with wear scar after impact abrasion wear test (figure 10).

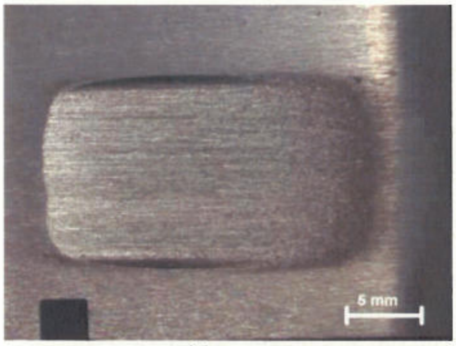

(a)

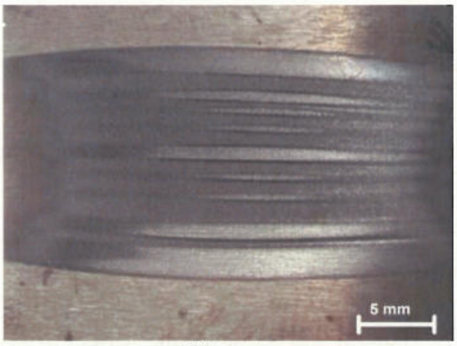

(b)

Figure 13. Top view of a typical wear scarf after a. ASTM B611 test, b. ASTM G65

CONCLUSION

The new wear test can distinctively predict accelerated wear of tough grades as well as potential chipping behavior of brittle grades when both abrasion and impact factors are involved. In general wear resistance increases with hardness. However, when testing bars, chipping occurs at the edges and leads to higher volume loss. SEM analysis shows an undamaged surface for brittle grades, while tough grades show binder pull out, grain cracking, dislodging, and micro abrasion. Dislocation steps causing plastic deformation are seen on large grains throughout the microstructure. Similar wear morphology is seen on a button taken from a rock drilling bit. It is also concluded that this test method can help in grade selection especially for grades with 84 HRA hardness or less used in oil and gas drilling, coal mining, road construction and other similar applications. ASTM B611 and G65 do not show distinctive volume losses for tough grades, and hence lack predicting the actual wear resistance for these grades. Also these two standard methods are not capable of showing the chipping behavior of very brittle grades that happens due to poor their resistance to impact. They only reveal resistance to abrasion and/or scratching. While the actual field test is time consuming and non-economical, this method is an alternative that can simulate both impact and abrasion engaged in down-hole drilling. This test is believed to be a more realistic laboratory method to predict impact abrasion behavior of cemented carbides.

FUTURE WORK

Primary test results show a good correlation between resistance to impact abrasion wear and hardness. However, bars may not be an optimum shape for testing. Most cobalt cemented carbide parts used in oil and gas drilling, coal mining, and road construction do not have a sharp angle presented in the tested parts. Hence, geometries closer to actual field application should also be considered. In order to expand test capabilities for various geometries, impeller design is modified to test buttons. Buttons can be conical, SRT, chisel, or any other commonly used designs in applications mentioned above. In addition, depending on the formation, rocks with different levels of abrasiveness can be provided for testing. Also, comparison of impact abrasion wear samples with actual buttons pulled out of drilling bits in various applications, different ROPs (rate of penetration), WOBs (weight on bit), and footage drilled will be considered.

ACKNOWLEDGEMENT

The authors are grateful to Bryan Brooks for conducting the experiments.

REFERENCES

1. S. Usmani and S. Sampath, "Effect of Carbide Grain Size on the Sliding and Abrasive Wear Behavior of Thermally Sprayed WC-Co Coatings", *Tribology transactions*, 1997, vol. 40, pp. 470-478.
2. P. H. Shipway, J. J. Hogg, "Dependence of Microscale Abrasion Mechanisms of WC-Co Hardmetals on Abrasive Type" *wear*, 2005, vol. 259, pp. 44-51.
3. J. Pirso, S. Letunovits and M. Viljus, "Friction and Wear Behavior of Cemented Carbides", *wear*, 2004, vol. 257, pp. 257-265.

Attachment #4

Paper: R. D. Wilson, J. A. Hawk (1999): *Impeller wear impact-abrasive wear test*. US Department of Energy, Albany Research Center, USA.

ELSEVIER

Wear 225–229 (1999) 1248–1257

WEAR

Impeller wear impact-abrasive wear test

R.D. Wilson, J.A. Hawk *

US Department of Energy, Albany Research Center, 1450 Queen Avenue SW, Albany, OR 97321, USA

Abstract

In order to more accurately simulate wear behavior that occurs in the field (i.e., impact coupled with abrasion), an impeller-in-drum wear test has been developed. The apparatus is similar to the one first developed by Bond; however, in the apparatus used at the Albany Research Center, three paddles instead of just one are situated in the drum which can be impacted and abraded during the course of the wear test. In using three paddles, a standard can be run at the same time as the specimens of interest. Two test procedures have been developed which provide information on the relative resistance of a material to the combined action of impact and abrasion. In the first procedure, the wear samples are run for 1 h on each side of the specimen paddle. This average value of the two tests gives an upper average limit to the impact-abrasive wear of the material, but has the advantages of being easy to run and relatively quick. The second procedure attempts to determine the steady-state wear behavior by running sequential wear tests on one surface of the specimen paddle. In this procedure, anywhere from three to five 1-h tests are run on one surface of the paddle. The cumulative mass or volume loss is plotted as a function of time and the slope of the linear portion of the curve provides the value for the steady-state wear rate. In addition to describing the experimental procedure, wear mechanisms will be discussed and the changes that occur in the microstructure as a result of the wear tests will also be described. The way various alloys behave in pure abrasion and in impact–abrasion will be discussed, highlighting the change in a material's wear behavior with a change in wear mode.

Keywords: Abrasion; Impact; Impeller-in-drum; Steel; Ferrous composite

1. Introduction

Bond [1] developed a laboratory scale test to accurately simulate the wear conditions that exist in the impact crushing of ores (both soft and hard) by impact hammers and blow bars. The rationale for the development of the test apparatus was to be able to predict the wear, and hence the energy consumption that occurred in the crushing and grinding of ore [2]. Bond's equation (i.e., the 'Third Theory') found that the energy input required to crush or grind rock is proportional to the square root of the new surface produced. Using his laboratory impact-pulverizing unit facilitated the calculation of the energy requirements needed to reduce a quantity of ore of a given starting size to a quantity of ore of the desired size. A critical factor is knowing the energy input to the driving motor, with due allowance made for frictional losses in the gears and bearings and the energy conversion efficiency of the motor. Once these factors are determined for the laboratory unit, conversion to a full-scale unit only requires a knowledge of the energy efficiency of the crushing or grinding unit in the field. For large units, the energy efficiency factor remains fairly constant. In reality, abrasive wear in ore processing is complicated by many factors other than energy consumption. However, the Bond approach has been very successful in predicting wear by applying a set of empirical formulas to an abrasion index, as determined in his laboratory wear test machine [2].

The machine Bond used for this test was an impact-pulverizer type in which 1.6 kg of screened ore (-19 mm $+ 12.5$ mm) were pulverized by impact with a rapidly rotating paddle made from a standard grade of steel (AISI 4325, hardened to 5.2 GPa (500 HB)). Wear of the paddle was measured in grams (to the nearest tenth of a mg). This wear constituted the abrasion index (A_i). The energy used in abrading the paddle was also calculated from the screen analysis of the feed and pulverized product, using the Bond work index equation [2,3]. From this, it is possible to calculate the wear on the paddle in terms of grams per kilowatt-hour. Multiplying the abrasion index by a constant (determined in conjunction with the full scale grinding or crushing machine of interest) gives the wear for an 'average' ore in terms of the mass of metal abraded per

* Corresponding author. Fax: +1-5419675845; E-mail: hawk@alrc.doe.gov

0043-1648/99/$ - see front matter
PII: S0043-1648(99)00046-0

kilowatt-hour. It is apparent that in using the Bond abrasion index to predict wear in crushing and grinding, the wear equation must be developed for each type of crushing or grinding machine. Bond was able to do this by correlating the reported wear and energy consumption from a large number of crushing and grinding operations with the abrasion index of the respective ores, as determined form his machine.

Subsequently, Paul and Hamel [4], building on the work started by French and Lissner [5], used a design of the Bond apparatus for making predictions of ore mill liner wear life. They too used the single paddle approach, but varied the test procedure, running multiple hour tests. In their research, ore passing a 25-mm screen but retained on a 12.5-mm screen was used as the feedstock. Variations in ore loading (0.4 and 0.8 kg charges) and ore particle size (−50 mm + 12.5 mm vs. −25 mm + 12.5 mm) were also investigated. Finally, the effects of dry vs. wet milling were examined. Correlations with field tests confirmed that the impeller-in-drum impact–abrasion test was a useful device for the quick prediction of abrasion resistance of liner materials when milling certain ores [4].

The Albany Research Center modified Bond's original impact pulverizer design so that the impeller hub assembly could hold three paddles instead of one. In this way, the impeller-in-drum wear apparatus can be utilized as a material wear testing device instead of a machine used solely for determining the abrasive index of ores. A holder with three paddle positions also allows triplicate samples to be run, or duplicate samples with a standard if one is required. The impeller-in-drum is used to determine the impact-abrasive wear rate for various materials, and is used in conjunction with the pin-on-drum (two-body abrasion), the dry-sand rubber-wheel (three body abrasion), and the jaw crusher (high-stress, gouging abrasion) in material correlation studies.

The impeller-in-drum creates an environment which possesses both impact events and abrasion. The size of the damage per impact–abrasion event on the surface of the wear specimens is quite a bit larger than that created either by the pin-on-drum or the dry-sand rubber-wheel, and the overall extent of damage is greater than either of these tests. Conversely, the intensity of the damage in the impeller-in-drum is less than that created in the jaw crusher, and the damage is less severe as well. In this way, this test procedure bridges the gap between the purely abrasive wear tests and the high-stress, gouging wear test.

This paper will discuss the general design of the impeller-in-drum and its operating procedures. Data generated from the test will be presented and the damage mechanisms will be discussed.

2. Experimental procedures

2.1. Impeller-in-drum apparatus and test specimens

The impeller–tumbler wear test apparatus uses an impeller-in-a-(rotating) drum arrangement (Fig. 1). The central impeller holds the three paddles which subsequently impact the ore media at a high linear velocity. The impeller and ore reside inside a nominally closed and slowly rotating larger drum. (A 3.0-mm gap exists between the covering plate and the drum, so that the smaller wear debris can escape the drum during operation.) When operating, the drum and the impeller rotate in the same direction. The large drum, which is rubber lined (to both reduce noise and to provide some friction between the drum and the ore), rotates slowly at 45 rpm, lifting the ore until it overcomes the frictional forces of the rubber lining and falls into the path of the rapidly rotating paddles. The impeller–tumbler wear test apparatus uses three metal paddles as wear test specimens instead of the one used in the Bond apparatus. These paddles are 75 mm × 25 mm × 12.5 mm. Approximately 38 mm of the length of the paddle extends from the impeller hub assembly and is

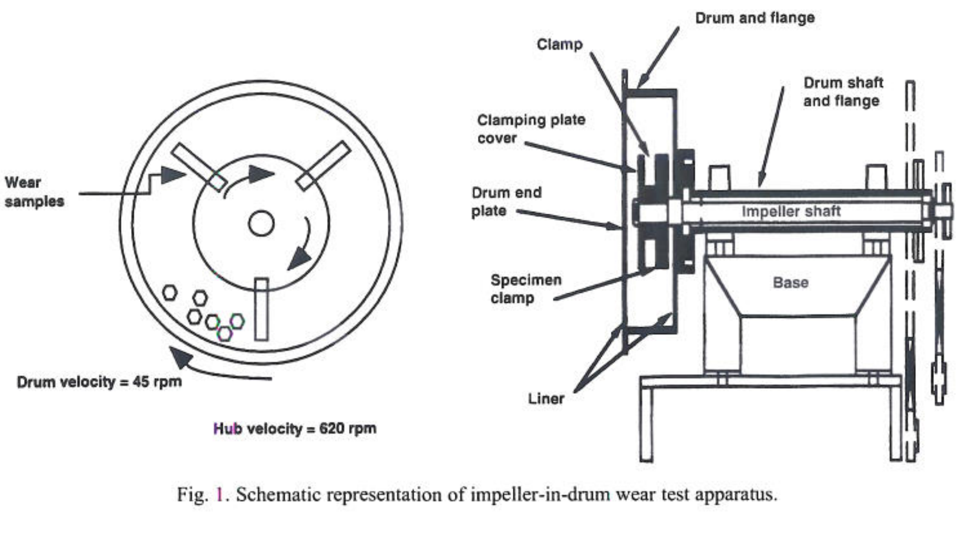

Fig. 1. Schematic representation of impeller-in-drum wear test apparatus.

available for particle impact. This translates into approximately 950 mm^2 of impact surface area. During operation the paddles rotate at 620 ± 5 rpm (a velocity equal to about 6 m/s at the tip of the paddle), causing them to impact against pieces of a hard abrasive mineral, for example, quartzite or granite or limestone. The ore-wear specimen impacts cause wear to occur on the broad faces of the paddles from a combination of impact-type events as well as from abrasion. The impeller–tumbler wear test provides quantitative information on the impact–abrasion wear rate of the three test specimens through measurements of the mass loss before and after the wear test schedule. Wear test variance is typically less than 10% for a duplicate set of specimens, although this test does have the potential for greater wear variance than either the dry-sand, rubber-wheel or the pin-on-drum. [1]

2.2. Impeller–tumbler test procedure

2.2.1. One-hour test procedure

The general test procedure for the impeller–tumbler starts with the sizing of ore in the range of −25 mm to +19 mm. After this step, 0.6 kg of ore are measured, and the number of particles that make up the charge is counted. Typically, for a 0.6 kg charge of high silica quartzite, the number of particles range from 38 to 44. The 0.6 kg charge is then loaded into the impeller, and the cover is bolted into place. An empty bag is positioned under the discharge chute, and catches any ore debris that escapes from the drum during operation and is not vented by the cyclone exhaust system. Note that there is a 3-mm gap between the cover and the drum, so that ore debris < 3 mm can continuously escape the drum during operation. Typically, 30 to 50 g of fines will escape from the drum during a 15-min milling run. The cyclone exhaust system collects and traps the very finest dust. In this way, only the larger ore fragment are comminuted in the drum.

The drum and impeller are then set into motion. This marks the beginning of the first of two 1-h tests. The speed of the impeller is adjusted to 620 rpm for the first 15-min interval. After the first 15-min test interval has elapsed, the impeller and drum are stopped, the cover is removed, and the ore is collected. A fresh 0.6 kg charge of ore is placed in the drum and the procedure is repeated for a second 15-min interval. This is done twice more, for a total running time of 1 h. The amount of ore passed through the impeller-in-drum system is 2.4 kg. After the first four 15-min tests, the paddle samples are removed, thoroughly cleaned, and then hot-air-dried. They are weighed to the nearest tenth of a milligram to determine the mass loss. The specimen face is then reversed, and a duplicate series of four 15-min tests are run. The results of these two series of tests are averaged and the standard deviation is calculated.

2.2.2. Multi-hour test procedure

In the multi-hour impeller-in-drum test, only one side of the sample is tested. In this case, four or five 1-h test segments are run on one side of the specimen paddle in the same manner as the single hour test. After each 1-h time period, the sample is removed, thoroughly cleaned, and weighed. It is then placed back into the impeller-in-drum and a second hour of tests are performed. In each case, fresh ore is placed in the drum at 15-min intervals. For a 4-h test, 9.6 kg of ore are processed, while for the 5-h test 12 kg of ore are comminuted.

The results of the multi-hour test are presented in graphical form in terms of the cumulative mass or volume loss for the specimen as a function of time. In this way, the 'steady state' wear impact–abrasion wear rate can be determined if one exists from the linear portion of the mass/volume loss vs. time curve.

3. Results and discussion

3.1. Microscopy and damage evolution of wear surfaces

Fig. 2 shows a series of scanning electron photomicrographs of the wear surface of a 304 SS test specimen. The top photomicrograph shows an area of the paddle furthest from the impeller hub (i.e., near the end of the paddle), the region that undergoes the most severe wear. Damage in this region is extensive and material has been worn away in small chunks (see the '*' region in Fig. 2a). There are also indications of abrasive wear. The middle photomicrograph is a region near the middle of the wear surface. Damage once again is extensive, but qualitatively not as severe as in the region near the end of the paddle. The bottom photomicrograph shows a single impact near the impeller hub. Damage in this region is sporadic. This image shows the type of damage a single ore particle imparts to the ductile material like the 304 SS. The impact has caused an uplifting of material to one side of the crater (a direct consequence of the oblique angle of impact of the ore particle). It is unknown how much material, if any, was lost from the specimen as a result of this single impact event, but a second and third impact in the general vicinity of the uplifted lip of material would most certainly detach it as a wear chip. It is hypothesized that the mechanisms of material removal in the impeller-in-drum has many similarities to that of erosive wear [6], except that the scale of damage is much greater. Abrasion of paddles occur when

[1] Precautions must also be exercised when using the impeller-tumbler wear test apparatus. The test causes a large amount of very fine particulate matter. For example, when working with high silica quartzite, ventilation through the use of an cyclone exhaust system, as well as through the use of a respirator or small particle dust mask is required. The silica-rich dust will irritate the mucus membranes in the throat and nasal passages in the short term and can cause silicosis, a form of lung cancer if exposed for longer times.

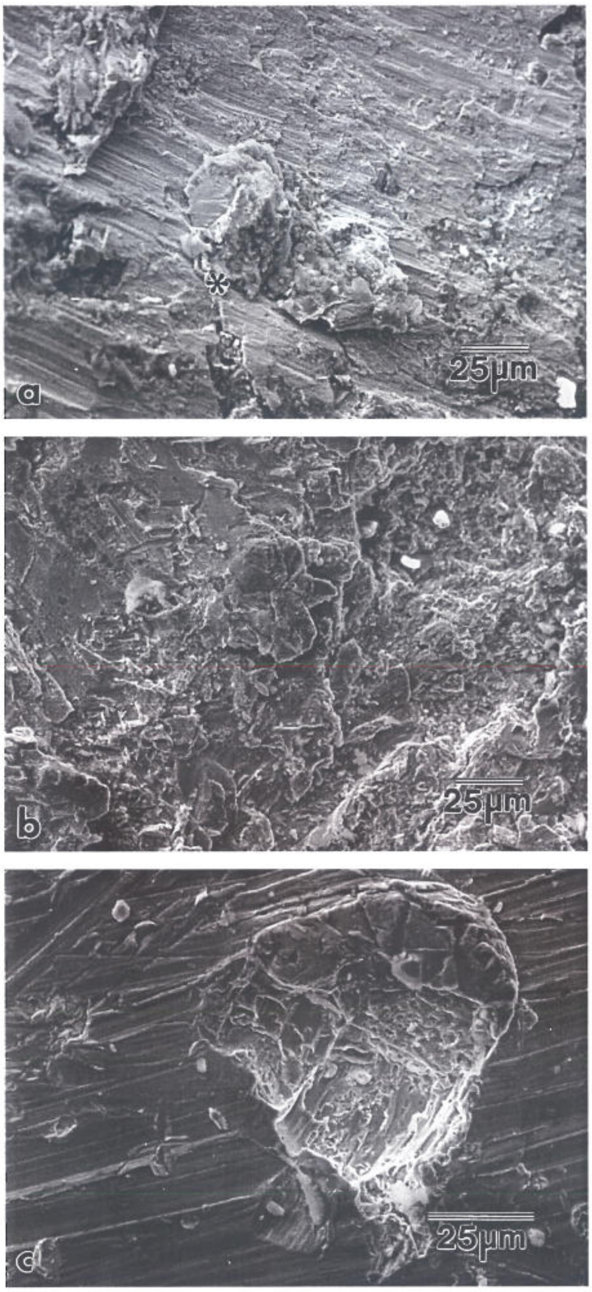

Fig. 2. Scanning electron photomicrographs of AISI 304 SS impacted and abraded against high-silica quartzite: (a) near tip of wear specimen; (b) near the middle area of the wear surface, and (c) near the impeller hub.

the ore particles impact the surface at shallow or glancing angles.

Fig. 3 shows a series of scanning electron photomicrographs from a P/M TiC reinforced ferrous composite. This composite is significantly harder than the 304 SS (9.3 GPa vs. 1.6 GPa), with the majority of the hardness increase a result of the high volume fraction of TiC particles. Even though this material is a composite, the material removal mechanisms are qualitatively similar. From examining the photomicrographs of a single impact to the composite, no significant differences exist from that found in the 304 SS. Specifically, no cracking was observed in and around the TiC reinforcement, although the depth of the crater appears to be shallower (note that the magnification in Fig. 2c is 750 × compared to the 500 × magnification in Fig. 3c).

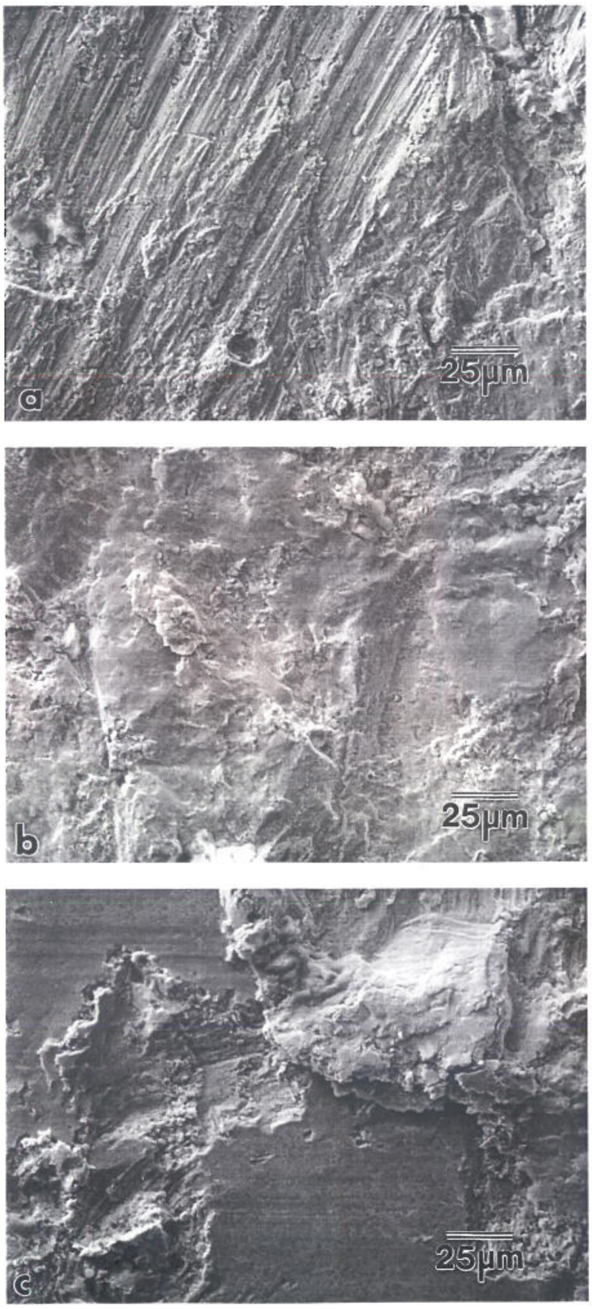

Fig. 3. Scanning electron photomicrographs of TIC particle reinforced composite impacted and abraded against high-silica quartzite: (a) near tip of wear specimen; (b) near the middle area of the wear surface; and (c) near the impeller hub.

Table 1
Typical impeller–tumbler wear data for ferrous alloys (wear rates determined from 1-h tests)

Alloy and designation	Chemical composition	Hardness (BHN)	Volume loss (mm^3/h)
304 SS	18.9Cr–2.4Mn–8.0Ni–0.4Si–0.3Mo–0.3Cu	153	104.7
Gall Tough®[a]	0.1C–16.3Cr–5.5Mn–5.2Ni–3.5Si–0.1Mo–0.1Cu–0.1N	184	83.1
13% Mn Steel	1.1C–0.4Cr–12.8Mn–0.2Ni–0.4Si	201	78.2
ASTM A514	0.2C–0.5Cr–1.4Mn–0.2Ni–0.3Si–0.2Mo0.4Cu	269	94.7
18-18Plus®[a]	0.1C–17.4Cr–17.7Mn–0.4Ni–0.5Si–1.0Mo–1.0Cu–0.5N	315	90.5
REM 500	0.3C–1.1Cr–0.6Mn–0.3Si–0.2Mo	495	91.3
AISI 4340	0.4C–0.8Cr–0.7Mn–1.8Ni–0.3Si0.3Mo	515	89.7
HT-6A[b]	0.3C–19.6Cr–0.1V–7.2Fe (bal Ni)	597	188.2
D2 tool steel	1.6C–13.7Cr–0.5Mn–0.2Ni–0.4Si–0.8Mo–0.8V	608	69.5
White cast iron	3.2C–15.3Cr–0.8Mn–0.5Ni–0.4Si–1.0Mo	698	67.1
CHW-45[b]	2.1C–5.4Cr–0.2Ni–1.5Mo–1.1V	709	106.6
AISI 1060	0.8C–0.4Mn	716	63.9
MS-5A[b]	0.9C–15.2Cr–5.4Ni–3.8Mo–4.8Co–0.1V	772	109.4
CM[b]	2.3C–11.1Cr–0.2Ni–2.8Mo–0.1V	852	73.3
C[b]	2.7C–2.9Cr–0.2Ni–3.1Mo–0.1V	990	46.3

[a] The Gall Tough® and the 18-18 Plus® are nitrogen-containing stainless steels produced by the Carpenter Technology.
[b] These materials are the Ferro-Tic® line of TiC reinforced composites produced by Alloy Technology International (HT-6A is a Ni-based matrix, while the others are Fe-based).

3.2. Wear results for one hour tests

3.2.1. Single hour impeller-in-drum wear tests

Typical impeller-in-drum wear results are found in Table 1 for a selection of alloys and composites. For the homogeneous ferrous alloys and composites tested, volume loss generally decreases as the hardness of the alloy increases. However, in cases where a hard, brittle second phase is found. such as in the Fe–TiC reinforced composites, increased wear rates are typically observed. This occurs

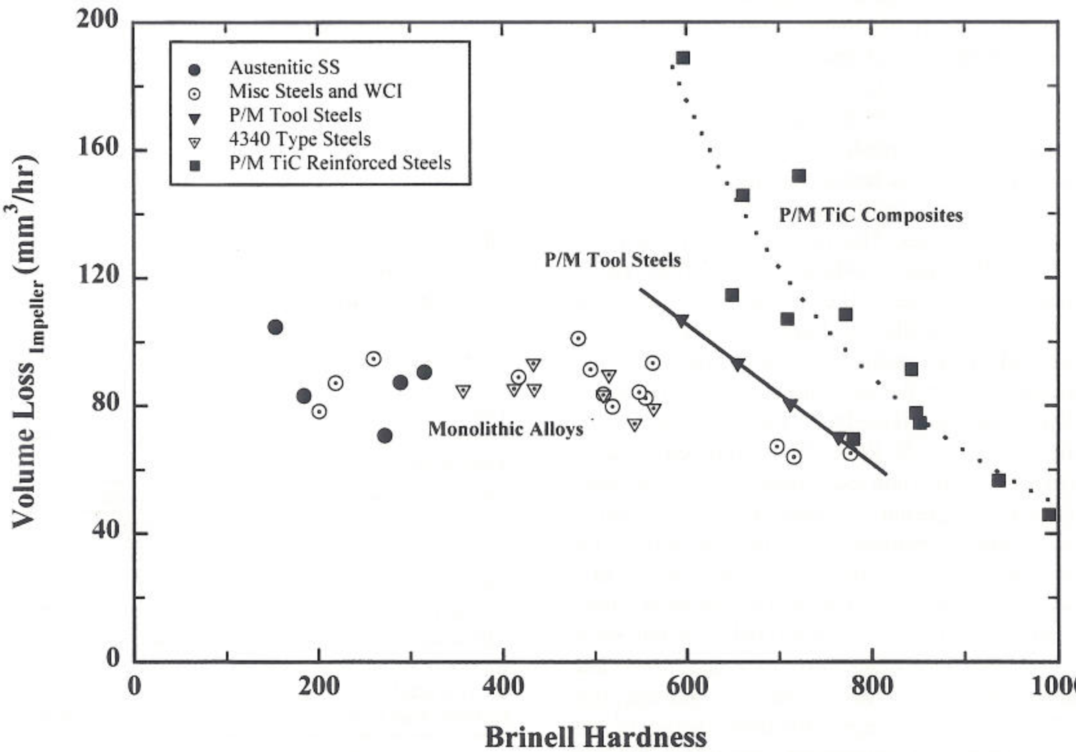

Fig. 4. Compilation of impeller-in-drum wear data for a variety of ferrous alloys and composites as a function of Brinell hardness. Data were generated from duplicate 1-h tests using, high-silica quartzite as the abrasive.

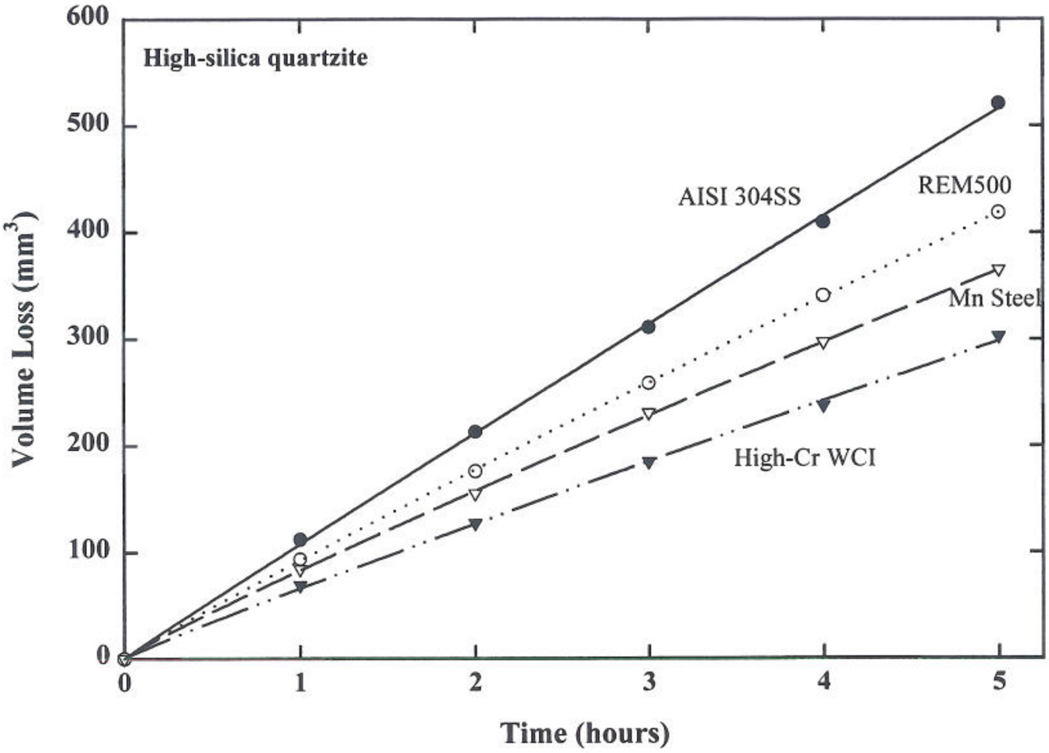

Fig. 5. Cumulative volume loss vs. time for AISI 304 SS, 12% Mn steel. REM 500 steel and a high-Cr white cast iron. Data were generated from sequential 1-h tests using high-silica quartzite as the abrasive.

because the second phase particles fracture as a result of the impact events, and if the matrix–particle bond is not good, fragments of the second phase are removed from the composite at an increased rate.

Fig. 4 shows a compilation of data for different type of materials tested in the impeller-in-drum. A variety of ferrous-based materials were tested, ranging from austenitic stainless steels to martensitic steels to P/M tool steels and TiC reinforced composites. The volume loss (in terms of mm^3/h) vs. Brinell hardness follows roughly three trends. The more homogeneous steels (i.e., the austenitic stainless steels, the martensitic steels, the high-Cr white cast irons and the cast tool steels) with hardness between 150 and 700 HB showed a slight decrease in wear with increasing hardness. This contrasts markedly to the wear behavior of the P/M tool steels and the P/M TiC reinforced composites. For these materials, and especially for the TiC-reinforced composites, a greater variation in volume wear is seen with a change in hardness. For these materials, the volume wear ranges from a high of ~ 190 mm^3/h to a low of ~ 45 mm^3/h, a 300% change. The hardness values change by only 67% (600 to ~ 1000 HB) over this same interval. The P/M tool steels also exhibited the same self-consistency in volume wear vs. hardness (dashed line in Fig. 4). The slope of the curve for these materials was not as steep as for the TiC-reinforced composites, but still much higher than the homogeneous alloys.

3.2.2. Multiple hour impeller-in-drum wear tests

A limited number of multi-hour tests have been run. Fig. 5 shows selected curves that were generated as a result of these tests for a number of alloys. From the linear portion of the volume wear vs. time curve, a steady-state wear rate can be determined. Table 2 contains the results of these calculations, where the initial wear rate (first hour of the test) is compared against the steady-state wear rate (slope of the curve at later times).

In looking at the data in Table 2, the 1-h wear rate overestimates the steady-state wear rate from a low value of 4.5% (ASTM A514 steel) to a high value of 20.4% (AISI 4340 steel). For the tests performed the average

Table 2
Compilation of steady state wear rates for impeller-in-drum impact abrasion test

Alloy and designation	Hardness (BHN)	Wear rate (mm^3/h)		Δ%
		1-h test	5-h test	
304 SS	153	112.2	102.3	−8.8
12% Mn Steel	208	84.2	69.7	−17.2
ASTM A514	269	101.3	96.7	−4.5
AISI 4340	515	96.2	76.6	−20.4
REM 500	476	93.7	81.0	−13.6
D2 Tool Steel	608	70.2	57.0	−18.8
Cr White Cast Iron	698	69.1	58.0	−16.1

Comparison is made to the wear rate of that material after the first hour of testing.

Table 3
Steady-state wear rates for ferrous alloys using different ore media

Alloy and designation	Hardness (BHN)	Wear rate (mm^3/h)		
		Quartzite	Limestone	Granite
304 SS	153	102.3	30.9	59.6
12% Mn Steel	208	69.7	19.1	27.3
ASTM A514	269	96.7	36.2	80.9

Results from 5-h impeller-in-drum wear tests.

overestimation was 14.2% ($\pm$5.7%). So the tendency in the wear rate to decrease with time from an initial high value after 1 h to a lower rate once the break-in period has occurred would yield an error on the safe side as far as endurance is concerned but this overestimation would necessarily be costly in terms of economics.

Several factors about the multiple hour impeller-in-drum wear tests need to noted. First, it is clear that most specimens possess a break-in period where the wear rate is significantly higher (> 13.5%) in the first hour of the test than for later times. This is especially true if an 'as-cast' surface is tested. Much of the break-in that occurs to the paddles consists of the edges being rounded through impact and abrasion. Although this may be thought of as an undesirable feature of the test, in most real life wear situations, component break-in occurs as the counter-faces seek to conform to each other. In earth moving or excavation equipment, the same type of break-in processes occur as edges of bucket teeth and scraper blades are rounded through their interaction with the surrounding environment. The nice feature about this test is that the processes of break-in and steady state wear can be differentiated, and a point is reached where the wear rate can be calculated from the linear portion of the volume loss–time curve. This has been done for the materials shown in Fig. 5, and is given in Table 2 along with the wear rates from the first hour of the test. What can be seen is that the 1-h tests provide an upper limit of the wear rate for this test as it incorporates both break-in and steady-state wear. At some later period, the steady-state wear rate becomes clearly evident, and in most instances, is lower than the initial wear rate.

3.3. Wear results for different ore media

A limited number of multi-hour wear tests have been run using different ores (in these tests limestone and a granitic ore were used). The wear results of this limited study are contained in Table 3. Fig. 6 shows the volume loss vs. time curves for the 304 SS impacted and abraded against the high silica quartzite, the limestone and the granitic ore.

Fig. 7 shows a series of scanning electron photomicrographs of the wear surfaces of the 304 SS after testing on the three minerals. Impact–abrasion on the quartzite and

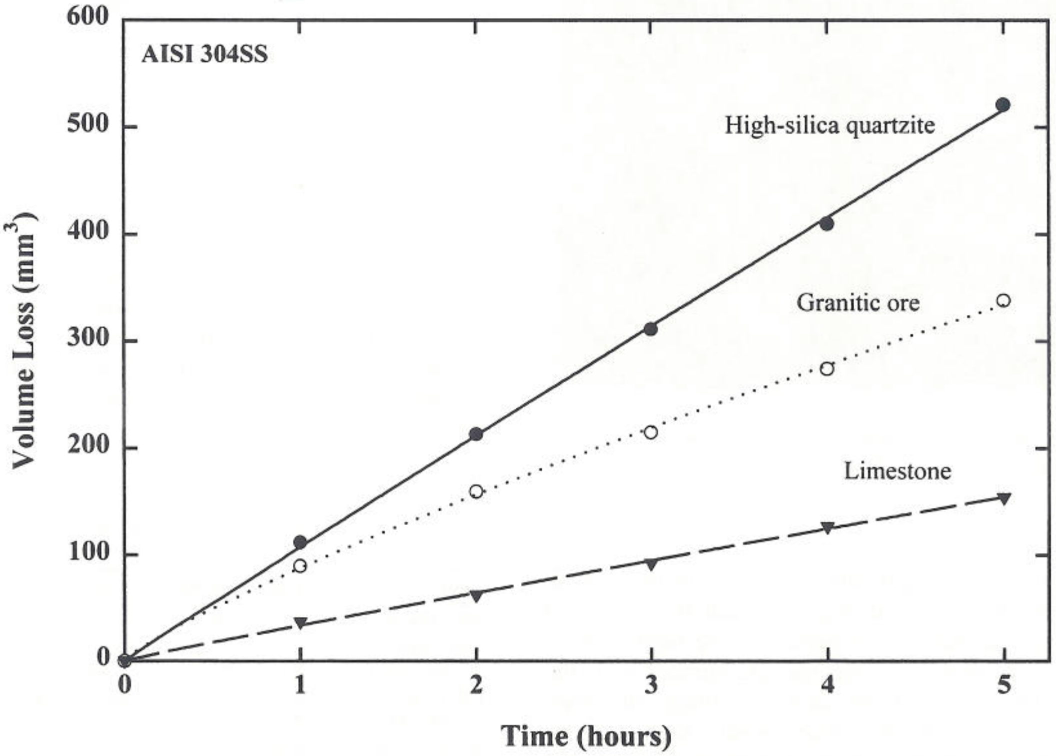

Fig. 6. Cumulative volume loss vs. time for AISI 304 SS impacted and abraded in sequential 1-h tests against high-silica quartzite, limestone and granitic ore.

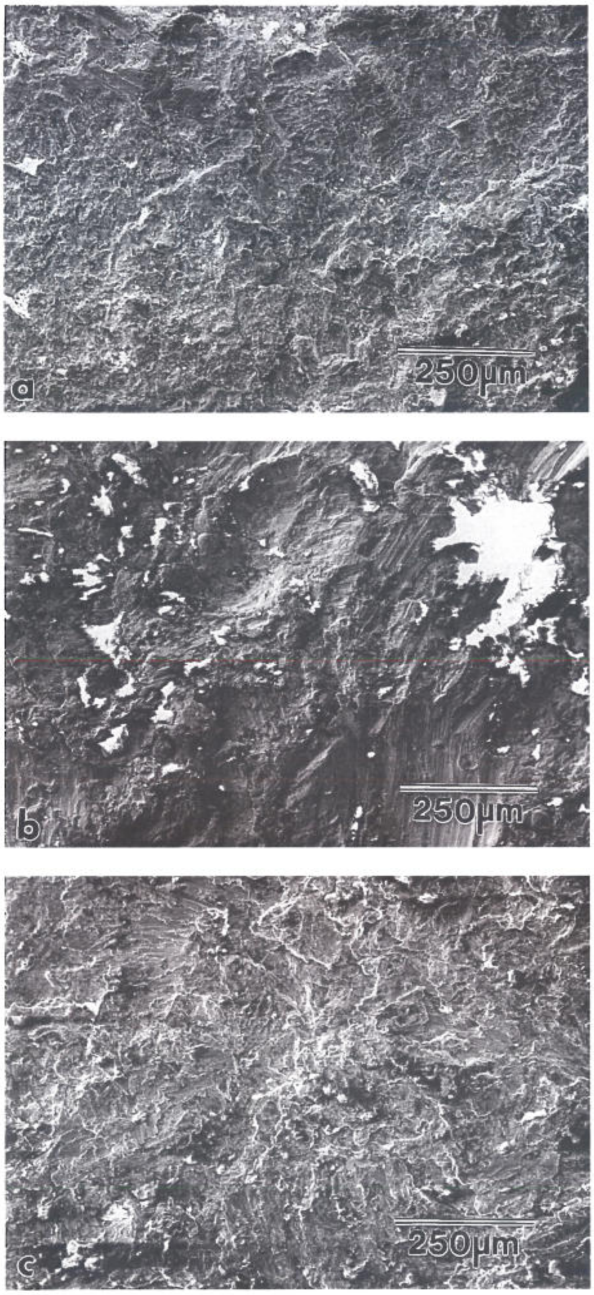

Fig. 7. Scanning, electron photomicrographs of AISI 304 SS impacted and abraded against (a) high-silica quartzite, (b) limestone, and (c) granitic ore. Test duration was 5 h in each case.

the granitic ore look qualitatively similar. In both cases, the amount and type of damage is much the same and there is some residual ore embedded in the wear surface. For the surface that was impacted and abraded with the limestone, there is much less uniform damage. However, there are regions where large grooves have been made by the ore. Also, much more of the limestone has been left embedded in the wear surface.

3.4. Work-hardening as a result of impact-abrasion

It has always been of interest to understand what happens to the near surface region of a material as a result of various wear processes. Most wear equations use the work-hardened surface hardness of the material as a variable, so knowledge of this number is useful in evaluating the wear behavior of a material. As a result, Vickers hardness measurements were made in conjunction with the multi-hour impact–abrasion wear tests. In the first series of experiments, Vickers hardness measurements were taken before and after a multi-hour impact–abrasion test. However, this did not tell us what was occurring in the interval between the starting condition and the final work-hardened state. Therefore, a second series of experiments were run where Vickers hardness measurements were taken both before wear testing and on the wear surface after each hour of testing. From these measurements, the work-hardening of the surface was monitored as a function of impact–abrasion wear time (or as a function of the amount of ore processed).

3.4.1. Surface hardness from impact–abrasion

In order to investigate the extent of work-hardening on a series of ferrous alloys, Vickers hardness measurements (1 kg load) were made on the wear surface of the paddle both before and after 5 h of impact–abrasion. A region approximately 12 mm from the free end of the sample was selected because the wear is fairly severe in this area. Hardness measurements were made before impact–abrasion testing and after sample testing was completed. After the samples were cleaned, dried and weighed, 600 grit SiC was used to abrade a smooth region on the sample for hardness measurements. The average and standard deviation of these measurements are contained in Table 4. It can be seen that in every case, the final work-hardened hardness exceeds the initial hardness. However, alloys that were in the hardened state to begin with (e.g., the 4340 steel), the relative increase in hardness of the near surface layer was minimal after testing. Alternatively, the 304 SS alloy, in the annealed condition, underwent an increase in hardness of 127% (Table 4). The other alloys tested showed hardness increases of between 17 and 26% (or $22.5 \pm 3.9\%$ on average).

Table 4
Effect of impact abrasion on the surface hardness of selected ferrous alloys

Alloy	Initial hardness	Final hardness	Δ%
AISI 304 SS	2.03 ± 0.03	4.60 ± 0.24	127
AISI 4340	5.29 ± 0.29	5.37 ± 0.29	2
D2 Tool Steel	6.85 ± 0.23	8.48 ± 0.11	24
REM 500	4.95 ± 0.10	6.24 ± 0.14	26
ASTM A514	2.51 ± 0.05	3.09 ± 0.05	23
White Cast Iron	6.48 ± 0.23	7.56 ± 0.30	17

Vickers hardness in GPa using a 1 kg load.

Table 5
Effect of impact abrasion on the surface hardness of selected ferrous alloys as a function of impact–abrasion time

Alloy	Initial hardness	Interval hardness					Δ_{f-i}%
		1st hour	2nd hour	3rd hour	4th hour	5th hour	
High-silica quartzite							
ASTM A514	2.75 ± 0.06	3.36 ± 0.21	3.32 ± 0.11	3.36 ± 0.15	3.47 ± 0.17	3.38 ± 0.14	23
AISI 304SS	3.20 ± 0.15	4.58 ± 0.19	4.84 ± 0.19	4.96 ± 0.13	5.09 ± 0.16	5.14 ± 0.10	61
12% Mn Steel	3.79 ± 0.18	6.41 ± 0.34	6.92 ± 0.24	6.94 ± 0.31	7.16 ± 0.23	7.25 ± 0.19	91
Limestone							
ASTM A514	2.90 ± 0.09	2.94 ± 0.07	3.32 ± 0.11	–	–	3.28 ± 0.12	13
AISI 304SS	3.28 ± 0.15	3.44 ± 0.25	4.13 ± 0.27	–	–	4.64 ± 0.18	41
12% Mn Steel	4.00 ± 0.15	4.85 ± 0.18	6.41 ± 0.14	–	–	6.53 ± 0.20	63
Granitic ore							
ASTM A514	2.78 ± 0.10	3.27 ± 0.08	3.10 ± 0.05	3.20 ± 0.08	–	3.39 ± 0.08	22
AISI 304SS	3.24 ± 0.10	4.47 ± 0.10	4.25 ± 0.12	4.65 ± 0.10	–	4.89 ± 0.18	51
12% Mn Steel	3.88 ± 0.25	5.75 ± 0.29	5.68 ± 0.14	6.10 ± 0.38	–	6.81 ± 0.20	76

Vickers hardness in GPa using a 1 kg load.

These experiments did not tell us much about what was happening, in between the start of the impeller-in-drum test cycle and its end. As such a series of three samples were run again and Vickers hardness measurements (1 kg load) were taken after each 1-h interval throughout the test cycle. After each hour of the impeller-in-drum wear test, the samples were thoroughly cleaned and weighed. The area where the original indents were made was then lightly abraded with 600 grit SiC, and another series of Vickers hardness indentations made. After this procedure, the sample was re-weighed and the next hour of testing completed. This was done for each of the 1-h time periods. These tests were performed for each of the ores available for use: high silica quartzite, limestone, and granite. The results of these measurements are shown in Table 5. These results show that the high-silica quartzite is the most aggressive ore of the three tested, wearing and work-hardening the surface of each alloy to a greater extent than either the limestone

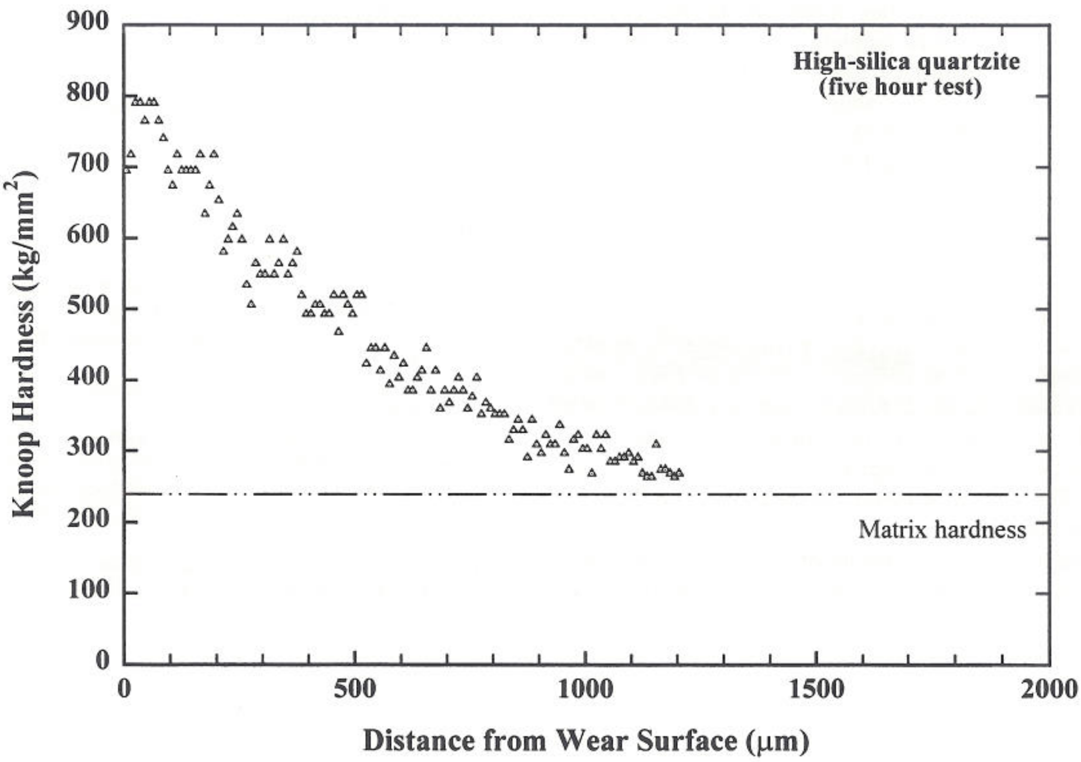

Fig. 8. Change in Knoop hardness with depth from the wear surface for a 12% Mn steel impacted and abraded against high-silica quartzite for 5 h.

or granitic ore. However, in each case, the alloy tested saw an increase in its hardness over the starting value.

In the case of the ASTM A514 steel, the hardness increased dramatically during the first hour of testing (2.8 to 3.4 GPa: ~96% of the total hardness increase), and remained at approximately that level for the remaining 4 h of testing. In the series of tests on the 304 SS, the hardness of the wear surface increased throughout the test. However, most of the hardness increase also occurred during the first hour of testing (~71% of the total hardness increase). The 12% Mn steel saw its surface hardness increase continuously during the 5-h test interval. As was seen with the other two alloys, most of its surface hardness increased during the first hour as well (~76% of the total hardness increase).

3.4.2. Extent of work-hardening

In order to investigate the depth of damage as a result of the impact-abrasion process, a cross-section of each of the three steels, the ASTM A514 steel, the 304 SS, and the 12% Mn steel, was cut, mounted, and polished using standard metallographic procedures. Micro-Knoop (50 g load) indentations were made from the wear surface into the bulk of the sample. The indentations into the bulk of the steel were made in 1 μm steps, offset 90° by 100 μm so as not to be influenced by the previous indentation. One set of data is shown in Fig. 8 for the 12% Mn steel impacted and abraded for 5 h using the high-silica quartzite. The Knoop hardness is very high near the surface (~7.8 GPa), but drops off quickly as measurements are made into the interior of the impeller specimen. In the example shown in Fig. 8, the bulk hardness is approached about 1.5 mm below the worn surface. For the ASTM A514 steel the bulk hardness is reached at about 0.2 mm below the worn surface. For the AISI 304 SS, the bulk hardness is also reached at a depth of about 1.5 mm.

4. Conclusions

The impeller-in-drum wear test simulates the impact-abrasion wear process. The 1-h test procedure is easy to perform but is labor-intensive compared to other typical laboratory wear tests (i.e., changing the ore media every 15 min). The test yields fairly reproducible wear rates (typically less than 10% between duplicate tests on the same sample). The 1-h test provides an upper limit on the wear rate for a material.

The multiple-hour impeller-in-drum wear test procedure provides a more realistic value of the wear rate of a material. The steady-state wear rate is determined from computing the cumulative mass or volume loss of a specimen vs. time, and then performing a least squares analysis of the data on the linear portion of the curve. This yields a value of the wear rate after break-in has occurred for the material. The 5-h test is considerably more labor-intensive than the duplicate 1-h test. However, the results may be more realistic in terms of what is actually occurring to the material, and this value may be more feasible to use when selecting a material for use in a given environment.

Since no commercially produced abrasive product is used in this test, the abrasive can be obtained from the quarry being mined or from the excavation site being cleared. Size of the starting ore is important, as it must be large enough to cause damage to the wear specimens in a reasonable amount of time to be useful as a laboratory test procedure. From this and previous studies [1–4], a size range of −25 mm + 19 mm works well for the current dimensions of the impeller-in-drum, producing measurable wear in a reasonable amount of time. Thus, the impeller-in-drum procedure lends itself to performing realistic laboratory wear studies.

Work-hardening of the wear surface is important in arriving at a realistic understanding of the wear process and rate. At the very least, the first hour of an impeller-in-drum wear test should be considered as the 'break-in' period, because the wear rate is highest and the majority of the work-hardening occurs during that time.

Acknowledgements

The authors would like to thank Dr. Ömer N. Doğan for performing the scanning electron microscopy investigation on these materials.

References

[1] F.C. Bond, Lab equipment and tests help predict metal consumption in crushing and grinding, Eng. J. 165 (1964) 169–175.
[2] F.C. Bond, The third theory of comminution, Min. Eng. 4 (1952) 484–494.
[3] F.C. Bond, New ideas clarify grinding principles, Chem. Eng. 69 (1962) 103–108.
[4] G. Paul, H.J.E. Hamel, A laboratory method for predicting ore mill liner life, South Afric. Mech. Engr. 20 (1970) 174–179.
[5] J.H. French, O.E. Lissner, Rotary mill liner practice in the South African gold mining industry, J. South Afric. Inst. Min. Met. 69 (1968) 77–102.
[6] A. Levy, Solid Particle Erosion and Erosion–Corrosion of Materials, ASM International, Materials Park, OH, 1995, pp. 13–25.

Attachment #5

Tumbling machine technical drawing

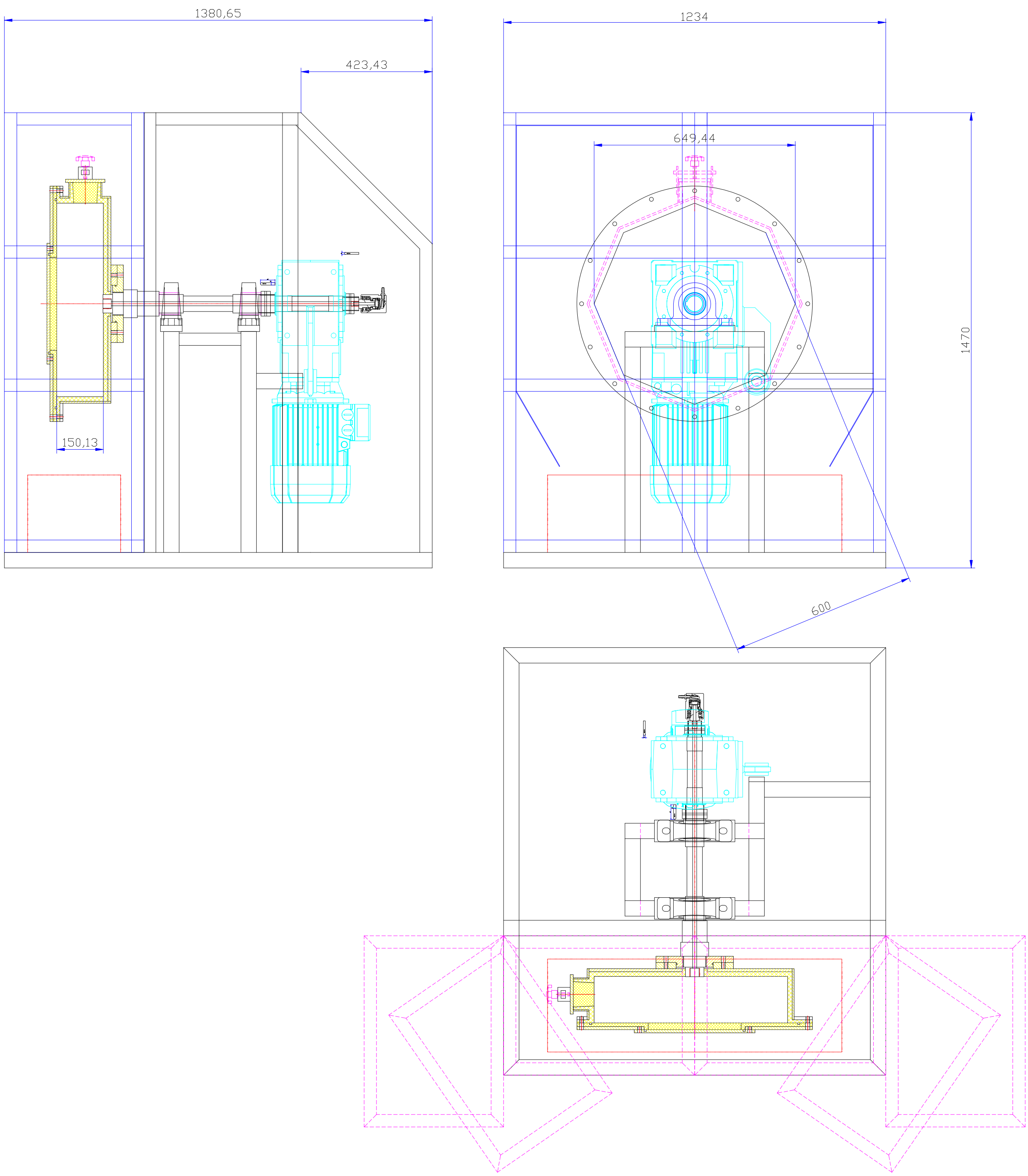
1380,65
423,43
150,13
1234
649,44
1470
600

Attachment #6

Press tool technical drawing

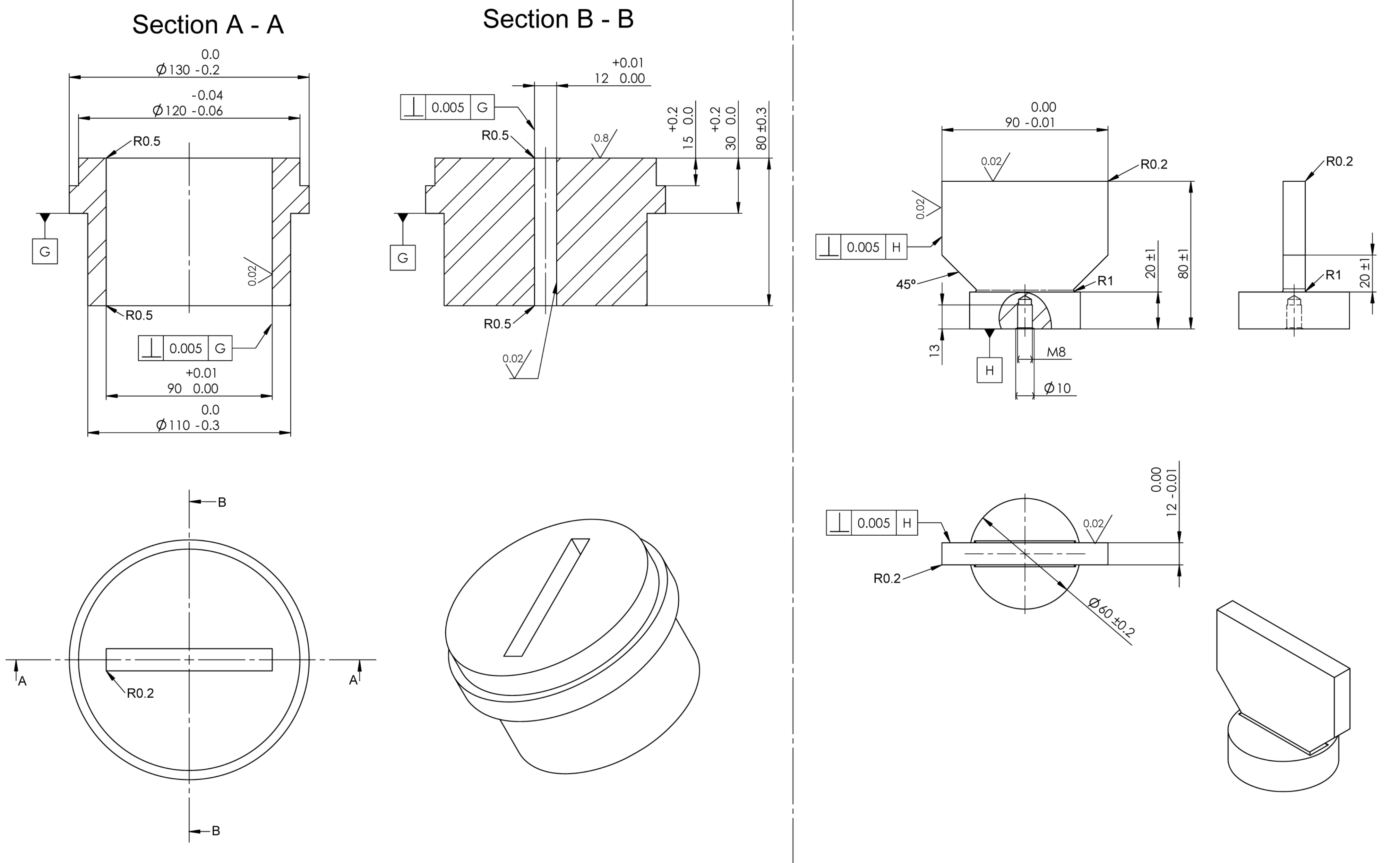

Ant. Quan	Det. nr. PartNo.	Benä mnin	Material: Steel	Det. ritn. nr/Anm. Part drg No./Remarks	Weight: 5.8 + 0.8 kg
Ritad Drawn: Carlos Filipe	Kontr. Checked	Name: 1350 K - m; Gen. tol.	Färdigvikt. Fin. wt. , kg	Smst. nr Gen drg. No. ,	
Datum Date: 17-11-08	Godk. Approved	Benämning Name: Cemented carbide paddle press tool 1x Table tool 2x Tool punch		Skala Scale: 1:2	
Atlas Copco				Ritn. nr Drg. No.	